



HAL
open science

Centered-potential regularization for the advection upstream splitting method

Martin Parisot, Jean-Paul Vila

► **To cite this version:**

Martin Parisot, Jean-Paul Vila. Centered-potential regularization for the advection upstream splitting method . SIAM Journal on Numerical Analysis, 2016. hal-01152395v1

HAL Id: hal-01152395

<https://inria.hal.science/hal-01152395v1>

Submitted on 16 May 2015 (v1), last revised 21 Sep 2016 (v2)

HAL is a multi-disciplinary open access archive for the deposit and dissemination of scientific research documents, whether they are published or not. The documents may come from teaching and research institutions in France or abroad, or from public or private research centers.

L'archive ouverte pluridisciplinaire **HAL**, est destinée au dépôt et à la diffusion de documents scientifiques de niveau recherche, publiés ou non, émanant des établissements d'enseignement et de recherche français ou étrangers, des laboratoires publics ou privés.

**CENTERED-POTENTIAL REGULARIZATION
FOR ADVECTION UPSTREAM SPLITTING METHOD:
APPLICATION TO THE MULTILAYER SHALLOW WATER MODEL
IN THE LOW-FROUDE NUMBER REGIME ***

MARTIN PARISOT[†] AND JEAN-PAUL VILA[‡]

Abstract. The current paper is devoted to the numerical resolution in multi-dimensional framework of a large class of models satisfying a conservation of energy. The proposed strategy is based on a regularized model where the advection velocity is modified by the gradient of the potential of the conservative forces in both mass and momentum equations. The numerical scheme is consistent with the asymptotic model when the ratio of the potential waves celerities are much larger than the material waves celerities, i.e. the so-called low-Mach number or low-Froude number regime depending on the application domain. In addition, the stability is ensured by the dissipation of energy, which act for mathematical entropy, even for large time step. More precisely, the CFL condition required for stability does not depend on the celerity of the potential waves. The main physical properties such as positivity, conservation of the total momentum and conservation of the steady state at rest are satisfied. Eventually, we propose several simulations to illustrate our results in the framework of the multilayers shallow-water equations.

Key words. conservation laws, non-conservative products, low-Mach number, low-Froude number, well-balanced scheme, entropy dissipation

AMS subject classifications. 35L60, 76M12, 86A05, 76E20, 35B40

DOI. XXXXX

1. Introduction. In the current paper, we are interested into system of L scalar unknowns $\rho_i(t, X) \in \mathbb{R}_+/\{0\}$ satisfying an advection equation with the velocity $U_i(t, X) \in \mathbb{R}^d$ subjected to irrotational force field defined from scalar potential $\phi_i(\rho, X) \in \mathbb{R}$ with $\rho = (\rho_1, \dots, \rho_L)^\top$, the space variable $X \in \Omega \subset \mathbb{R}^d$ and the time variable $t \geq 0$. The advection model reads

$$(M_{t,\varepsilon}) \quad \begin{cases} \partial_t \rho_i + \nabla \cdot (\rho_i U_i) & = 0 \\ \partial_t (\rho_i U_i) + \nabla \cdot (\rho_i U_i \otimes U_i) & = -\frac{\rho_i}{\varepsilon^2} \nabla \phi_i \end{cases}$$

with a given initial condition $\rho_i(0, X) = \rho_i^0(X) > 0$ and $U_i(0, X) = U_i^0(X)$. In the current study, we only consider periodic domains Ω of the d-dimensional space \mathbb{R}^d or bounded domain with no-flux boundary condition such that the first equation of $M_{t,\varepsilon}$ leads to a global conservation, so-called mass conservation. In the following, we refer to the scalar unknowns ρ_i as the mass and the second equation of $M_{t,\varepsilon}$ as the momentum balance. From now on, we denote by $|\Omega|$ the measure of the domain Ω . The parameter ε is the dimensionless number characterizing the ratio between inertial and potential force. In addition we define the potential energy $\mathcal{E}(\rho, X)$ such that

*Received by the editors XXXXX; accepted for publication (in revised form) XXXXX; published electronically XXXX.

<http://www.siam.org/journals/sinum/XXXXX.html>

[†] INRIA, ANGE Project-Team, Rocquencourt, F-78153 Le Chesnay Cedex, France; CEREMA, F-60280 Margny-Lès-Compiègne, France; CNRS, UMR 7598, Laboratoire Jacques-Louis Lions, F-75005, Paris, France; Sorbonne Universités, UPMC Univ Paris 06, UMR 7598, Laboratoire Jacques-Louis Lions, F-75005, Paris, France (martin.parisot@inria.fr)

[‡]Institut de Mathématiques de Toulouse, UMR CNRS 5219, INSA, F-31077 Toulouse, France (vila@insa-toulouse.fr)

$\partial_{\rho_i} \mathcal{E} := \phi_i$, the kinetic energy $\mathcal{K}_i := \frac{\rho_i}{2} \|U_i\|^2$ and the mechanical energy of the model $E := \frac{\mathcal{E}}{\varepsilon^2} + \sum_{i=1}^L \mathcal{K}_i$. For most of physical systems, the following assumption is fulfilled.

HYPOTHESIS 1.1. *The hessian $\mathbf{H}(\boldsymbol{\rho}, X)$ of the potential energy \mathcal{E} , defined by $\mathbf{H}_{ij} = \partial_{\rho_j}^2 \mathcal{E} = \partial_{\rho_j} \phi_i$, is positive-definite.*

Let us highlight the main properties of the model $M_{t,\varepsilon}$. First of all, the mechanical energy E satisfies the following dissipation law, with the equality case when the solution is regular

$$(1.1) \quad \partial_t E + \sum_{i=1}^L \nabla \cdot \left(\left(\rho_i \frac{\phi_i}{\varepsilon^2} + \mathcal{K}_i \right) U_i \right) \leq 0.$$

In addition, we consider the particular case where potential energy satisfies the following assumption.

HYPOTHESIS 1.2. *The potential is a symmetric linear application of the mass vector, i.e. $\boldsymbol{\phi} = \mathbf{H}\boldsymbol{\rho}$ with the hessian \mathbf{H} constant and symmetric, i.e. $\mathbf{H}_{ij} = \mathbf{H}_{ji}$.*

Then the total momentum satisfies the following conservation law

$$(1.2) \quad \partial_t \left(\sum_{i=1}^L \rho_i U_i \right) + \nabla \cdot \left(\sum_{i=1}^L \left(\rho_i U_i \otimes U_i + \frac{\rho_i \phi_i}{2\varepsilon^2} \mathbf{I}_d \right) \right) = 0.$$

Eventually, the solution of $M_{t,\varepsilon}$ satisfies many steady states, generally hard to estimate. As it was generally the case in the literature [4, 6, 17, 32, 35], we only consider the steady state at rest, i.e. with the additional condition $U_i = 0$. At the steady state at rest, the solution is characterized by a constant potential for each mass, i.e.

$$(1.3) \quad \phi_i(\boldsymbol{\rho}(t, X), X) = \bar{\phi}_i.$$

Many classical models of fluids mechanics based on Hamilton's principle can be written under the form $M_{t,\varepsilon}$. The case of one mass system, i.e. $L = 1$, corresponds to the isentropic Euler equations [16, 39, 41, 44] and in the framework of free surface flow to the classical shallow water model [13]. The non-isentropic Euler equations [24, 29] required another scalar equation, acting for the energy. Similarly, the hydrodynamic equations can be coupled with a system of equations modeling the forces evolution, such for plasma physic [12] or chemotaxis modeling [31]. However the numerical strategy proposed in the following can be adapted in such cases with no more difficulties. The numerical resolution of such models is generally based on the conservative form of the system, since the momentum equation of $M_{t,\varepsilon}$ can be replaced by the conservation law (1.2), see [36]. However, the preservation of the equilibrium in the case of potential ϕ_i non-linear or non-symmetric becomes a challenge and leads to the specific studies already cited.

For multi coupled-system, i.e. $L > 1$, the most obvious physical systems which can be written under the form $M_{t,\varepsilon}$ are the mixture of component [5], bipolar Euler-Poisson equations [11] and the multilayer shallow water model [3, 27, 33, 38]. Let us clarify the unknowns signification in the case of the multilayer shallow water model. The so-called mass $\rho_i > 0$ corresponds to the effective mass of the i^{th}

layer $\varrho_i h_i$ with ϱ_i the density of the fluid and h_i the layer thickness. The velocity $U_i \in \mathbb{R}^2$ corresponds to the horizontal velocity. Adopting the convention that the layers are numbered from the free surface to the bottom, the potential could be interpreted as the physical pressure in the layer and is given by $\phi_i = g \left(z_b + \sum_{j=1}^L \frac{\varrho_j h_j}{\varrho_{\max(i,j)}} \right)$, with z_b the bottom elevation. The related potential energy is given by $\mathcal{E} = g \sum_{i=1}^L \left(\left(z_b + \frac{1}{2} \sum_{j=1}^L \frac{\varrho_j h_j}{\varrho_{\max(i,j)}} \right) \varrho_i h_i \right)$ and the hessian $\mathbf{H}_{ij} = \frac{g}{\varrho_{\max(i,j)}}$ is constant and symmetric. Note that the hessian is positive-definite iff the layers are well-stratified, i.e. $\varrho_i < \varrho_{i+1}$. This assumption is required to ensure the multilayer shallow water model hyperbolic, see [15, 30], even if it is not a sufficient condition. In addition, in the case of flat topography, i.e. $z_b = 0$, the potential is a symmetric and linear function of the water thickness and the multilayer shallow water model satisfy the conservation law (1.2) so-called in this context conservation of the momentum of the column of water.

In the following work, we focus on the resolution of the advection model $M_{t,\varepsilon}$ with a small parameter ε . We assume that the forces satisfy the following condition.

HYPOTHESIS 1.3. *The hessian is well-conditioned independently of ε , i.e. $\kappa(\mathbf{H}) = O_{\varepsilon \rightarrow 0}(1)$ with $\kappa(\mathbf{H})$ the condition number of \mathbf{H} .*

Then two asymptotic models seem relevant, accordingly to the time scale, i.e.

- For small time scale $t = \varepsilon\tau$, the advection model $M_{\tau,\varepsilon}$ tends to a system of wave equations, see [43], i.e.

$$(M_{\tau,0}) \quad \left\{ \partial_{\tau\tau}^2 \tilde{\rho}_i - \nabla \cdot \left(\tilde{\rho}_i \nabla \tilde{\phi}_i \right) = 0 \right.$$

with the initial condition given by $\tilde{\rho}_i(0, X) = \rho_i^0(X)$ and $\partial_\tau \tilde{\rho}_i(0, X) = 0$ and $\tilde{\phi}_i(\tilde{\rho}, X)$ is the second order perturbation of the potential $\varepsilon^2 \phi_i(\tilde{\rho}, X) = \phi_i(\tilde{\rho}, X) - \frac{1}{|\Omega|} \int_\Omega \phi_i(\tilde{\rho}, X) \, dX$.

- For large time scale, the advection model $M_{t,\varepsilon}$ tends to the divergence free model

$$(M_{t,0}) \quad \left\{ \begin{array}{l} \nabla \cdot (\bar{\rho}_i \bar{U}_i) = 0 \\ \partial_t \bar{U}_i + (\bar{U}_i \cdot \nabla) \bar{U}_i = -\nabla \bar{\phi}_i \end{array} \right.$$

with the initial condition $\bar{U}_i(0, X) = U_i^0(X)$. See [23, 24, 25, 28] for the mono-system case $L = 1$. The parameters $\bar{\rho}_i(X)$ are defined by the average value of the potential at the initial condition, i.e. $\phi_i(\bar{\rho}, X) = \frac{1}{|\Omega|} \int_\Omega \phi_i(\rho^0, X) \, dX$ and $\bar{\phi}_i(t, X)$ act for Lagrange multiplier to satisfy the divergence free constrain.

Few comments about the formal derivation of the asymptotic models are briefly presented in Section 3. For more details about derivation and analysis of the asymptotic models, we refer to the cited works. The purpose of this work is to propose a numerical strategy able to solve $M_{t,\varepsilon}$ at the different regime of ε and satisfying the physical properties such are the dissipation of the mechanical energy (1.1), the conservation of the total momentum (1.2) and the steady state at rest (1.3) for both initial model $M_{t,\varepsilon}$ and asymptotic models $M_{\tau,0}$ and $M_{t,0}$.

For multi coupled-system, i.e. $L > 1$, the conservation law (1.2) can not replace the momentum balance of $M_{t,\varepsilon}$ since we can not written as much conservation laws than momentum balance equations. Several numerical strategies can be cited to adapt the Riemann solvers to the non-conservative hyperbolic equation, see [1, 8, 10]. However, the eigenvalues required for many numerical resolution of hyperbolic equations are hard to estimate in the case of a large number of equations. For example, the multilayer shallow water model is only hyperbolic under conditions, and the estimation of the eigenvalues is obtained only for the weakly stratified flows, i.e. $0 < 1 - \frac{\rho_i}{\rho_{i+1}} \ll 1$, see [28, 30]. In addition, the Riemann solvers are well-known to be too much dissipative in the asymptotic regime $\varepsilon \ll 1$, and required a very restrictive CFL condition, see [14].

In the current paper, we propose a numerical strategy to generalized the recent works [18, 34]. The numerical strategy is based on a centered discretization of the potential which leads to several advantages, i.e. the conservation of the total momentum (1.2), the steady state at rest (1.3) and the asymptotic regime $M_{\tau,0}$ and $M_{t,0}$ are naturally recovered at the discrete level. The stability of the scheme is ensured by a regularization of the mass flux involving the centered potential discretization. This strategy does not required the estimation of the eigenvalues of the system and imply a CFL condition not restrictive for small ε .

The present paper is organized as follow. In Section 2, we describe the numerical scheme and we perform the main analysis for large enough ε . The stability result and the truncation orders will be proved and commented. In Section 3, we briefly recall the derivation of the asymptotic model $M_{\tau,0}$ and $M_{t,0}$. Then we identify the asymptotic schemes in the corresponding regime and we proof the consistency in each cases. Eventually, in Section 4, we propose several numerical tests to illustrate the announced results.

2. Centered-potential regularization of AUS method. In the following section, we propose an adaptation of the so-called *Advection Upstream Splitting Method* (AUSM) introduced in [26]. The numerical strategy proposed in the following, from now on called *Centered-Potential Regularization* (CPR), generalize the method for any advection models such that the hessian of the energy potential is positive-definite. It is based on a centered estimation of the non-conservative term, as it is recommended in [14] to preserved the asymptotic limit, see section 3. In addition, we show in Section 2.3 that the centered estimation ensure the conservation at the discrete level of the total momentum (1.2) and the discrete stability of the steady state at rest (1.3). Then, the advection term of the momentum equation is discretized using an upwind scheme accordingly to the sign of the mass flux. This strategy ensure the dissipation of the kinetic energy (see Lemma 2.3). Eventually, the stability of the scheme is ensured by introducing a regularizing term in the numerical mass flux following the strategy introduced in [18, 34].

We consider a tessellation of \mathbb{R}^2 , denoted \mathbb{T} , composed of star-shaped control volumes. For any control volume $k \in \mathbb{T}$, we design its volume by $|k|$, its area by $|\partial k|$ and the set of its faces by \mathbb{F}_k . In addition, for any face $f \in \mathbb{F}_k$, we denote by $|f|$ its area, by $k_f \in \mathbb{T}$ the neighbor of k such that $k \cap k_f = f$ and by N_f^k the unit normal to the face f outward to the control volume k . Eventually we define the space step $\Delta x_k = \frac{|k|}{|\partial k|}$ and the normalized face size $\mu_f^k = \frac{|f|}{|\partial k|}$. We introduce a time step Δt such

that the numerical unknowns are estimated at time $t^{n+1} = t^n + \Delta t$. The numerical strategy presented below is based on a cell-centered finite volume method, i.e. the numerical unknowns at the time t^n are the approximation in each control volume $k \in \mathbb{T}$ of the averaged value of the mass $\rho_{i,k}^n > 0$ and of the velocity $U_{i,k}^n \in \mathbb{R}^d$. We also introduce the discretization of the potential $\phi_{i,k}^n := \phi_i(\rho_k^n, X_k)$ and the centered symmetric notations for any face $f \in \mathbb{F} = \bigcap_{k \in \mathbb{T}} \mathbb{F}_k$

$$\begin{aligned} 2\rho_{i,f}^n &:= \rho_{i,k}^n + \rho_{i,k_f}^n & \text{and} & & 2\rho_{i,f}^{n+1}U_{i,f}^n &:= \rho_{i,k}^{n+1}U_{i,k}^n + \rho_{i,k_f}^{n+1}U_{i,k_f}^n \\ 2\phi_{i,f}^n &:= \phi_{i,k}^n + \phi_{i,k_f}^n & \text{and} & & 2\delta\phi_{i,f}^n &:= \left(\phi_{i,k_f}^n - \phi_{i,k}^n\right) N_f^k. \end{aligned}$$

We used an Implicit-Explicit (IMEX) time discretization, i.e. the numerical flux is estimated using the mass approximation at time iteration $n+1$ and the approximation of the velocity at time iteration n . The numerical scheme of the mass conservation $M_{t,\varepsilon}$ reads as follow

$$(2.1) \quad \rho_{i,k}^{n+1} = \rho_{i,k}^n - \frac{\Delta t}{\Delta x_k} \sum_{f \in \mathbb{F}_k} \mathcal{F}_{i,f}^{n+1} \cdot N_f^k \mu_f^k$$

where the numerical mass flux $\mathcal{F}_{i,f}^{n+1}$ is an approximation of $\frac{1}{|f|\Delta t} \int_{t^n}^{t^{n+1}} \int_f \rho_i U_i d\sigma dt$. Then, the momentum balanced $M_{t,\varepsilon}$ is approximated using an explicit time discretization where the space advection is estimated using an up-wind flux following the direction of the numerical mass flux. It reads

$$(2.2) \quad \begin{aligned} \rho_{i,k}^{n+1}U_{i,k}^{n+1} &= \rho_{i,k}^n U_{i,k}^n - \frac{\Delta t}{\Delta x_k} \rho_{i,k}^{n+1} \sum_{f \in \mathbb{F}_k} \frac{\phi_{i,f}^{n+1}}{\varepsilon^2} N_f^k \mu_f^k \\ &\quad - \frac{\Delta t}{\Delta x_k} \sum_{f \in \mathbb{F}_k} \left(U_{i,k}^n \left(\mathcal{F}_{i,f}^{n+1} \cdot N_f^k \right)^+ - U_{i,k_f}^n \left(\mathcal{F}_{i,f}^{n+1} \cdot N_f^k \right)^- \right) \mu_f^k. \end{aligned}$$

where we use the positive and the negative part functions $2(\psi)^\pm = |\psi| \pm \psi \geq 0$. In the current work, the numerical mass flux is defined from the centered discharge regularized using the centered potential variation, i.e.

$$(2.3) \quad \mathcal{F}_{i,f}^{n+1} := \rho_{i,f}^{n+1} \left(U_{i,f}^n - \frac{\gamma \Delta t}{\varepsilon^2} \frac{\delta\phi_{i,f}^{n+1}}{\Delta x_{i,f}^{n+1}} \right)$$

with the regularization coefficient $\gamma \geq 0$ and the space step at the face defined by

$$2 \frac{\rho_{i,f}^{n+1}}{\Delta x_{i,f}^{n+1}} := \frac{\rho_{i,k}^{n+1}}{\Delta x_k} + \frac{\rho_{i,k_f}^{n+1}}{\Delta x_{k_f}}.$$

Assuming the mass are positive, the space step at faces $\Delta x_{i,f}^{n+1}$ is bounded by the space step of the neighboring control volume Δx_k and Δx_{k_f} . In addition, for regular grid, i.e. for any $k \in \mathbb{T}$ we have $\Delta x_k = \Delta x$, the space step at the faces is constant, more precisely $\Delta x_{i,f}^{n+1} = \Delta x$. In the following, we will see that the CPR scheme (2.1)-(2.2)-(2.3) has interesting properties such as mechanical energy dissipation (1.1), conservation of the total momentum (1.2) and well-balanced (1.3) under the following CFL-like condition.

HYPOTHESIS 2.1 (CFL-like condition). *Assume that the time step Δt is small enough such that for any face f , the following inequality is fulfilled*

$$\sum_{f \in \mathbb{F}_k} \left| \mathcal{F}_{i,f}^{n+1} \cdot N_f^k \right| \mu_f^k \frac{\Delta t}{\Delta x_k} < \rho_{i,k}^n.$$

PROPOSITION 2.1 (Positivity). *Assume that the mass at the initial condition $\rho_{i,k}^0$ are positive. Then there exists a time step Δt such that the CFL-like condition (Hypothesis 2.1) is fulfilled and the mass approximations $\rho_{i,k}^n$ are positive.*

Proof. Assume that the mass approximation at time iteration n is positive, i.e. $\rho_{i,k}^n > 0$, which is true at the initial condition. The CFL-like condition (Hypothesis 2.1) is clearly satisfied for $\Delta t = 0$ and it is not an equality case. Then since the mass approximations $\rho_{i,k}^{n+1}$ are continuous functions of the time step Δt , there exists a neighborhood of 0 for Δt such that the condition is satisfied.

By direct estimation, we have

$$\rho_{i,k}^{n+1} = \rho_{i,k}^n - \frac{\Delta t}{\Delta x_k} \sum_{f \in \mathbb{F}_k} \mathcal{F}_{i,f}^{n+1} \cdot N_f^k \mu_f^k > 2 \frac{\Delta t}{\Delta x_k} \sum_{f \in \mathbb{F}_k} \left(\mathcal{F}_{i,f}^{n+1} \cdot N_f^k \right)^- \mu_f^k$$

which leads to the positivity of the mass approximations $\rho_{i,k}^{n+1}$. \square

To compare the CFL-like condition (Hypothesis 2.1) to classical one, let us write a more restrictive CFL-like condition in a more classical form. We overestimate the numerical mass flux by

$$\left(\mathcal{F}_{i,f}^{n+1} \cdot N_f^k \right)^- \leq \rho_{i,f}^{n+1} \left(|U_{i,f}^n \cdot N_f^k| + \gamma \frac{\Delta x_k}{\varepsilon^2} \frac{|\delta \phi_{i,f}^{n+1}|}{\Delta x_{i,f}^{n+1}} \frac{\Delta t}{\Delta x_k} \right).$$

Since the sum over the faces is normalized, the CFL-like condition can be estimated by face and leads to a second order polynomial function $\left(V_2 \frac{\Delta t}{\Delta x_k} \right)^2 + V_1 \frac{\Delta t}{\Delta x_k} - 1$ with

$$V_1 = 2 \frac{\rho_{i,f}^{n+1}}{\rho_{i,k}^{n+1}} |U_{i,f}^n \cdot N_f^k| \quad \text{and} \quad V_2 = \sqrt{2 \gamma \frac{\rho_{i,f}^{n+1}}{\rho_{i,k}^{n+1}} \frac{\Delta x_k}{\varepsilon^2} \frac{|\delta \phi_{i,f}^{n+1}|}{\Delta x_{i,f}^{n+1}}}.$$

which is negative when $(V_1 + V_2) \frac{\Delta t}{\Delta x_k} < 1$. Since the mass $\rho_{i,k}^{n+1}$ are positive under the CFL condition, the space length $\min(\Delta x_k, \Delta x_{k_f})$ is a lower bound of $\Delta x_{i,f}^{n+1}$. In addition, the centered-value $\rho_{i,f}^{n+1}$ is larger than $\min(\rho_{i,k}^{n+1}, \rho_{i,k_f}^{n+1})$. Eventually, using the previous simplifications, we get the following CFL-like condition

$$(2.4) \quad \left(|U_{i,f}^n \cdot N_f^k| + \sqrt{\frac{\gamma}{2}} \sqrt{\frac{|\delta \phi_{i,f}^{n+1}|}{\varepsilon^2}} \right) \frac{\Delta t}{\min(\Delta x_k, \Delta x_{k_f})} < \frac{\min(\rho_{i,k}^{n+1}, \rho_{i,k_f}^{n+1})}{2 \rho_{i,f}^{n+1}}.$$

which is more restrictive than Hypothesis 2.1. We recall that classical Godunov scheme are generally stable under a CFL condition with the form, see [36]

$$(2.5) \quad \left(|U_{i,f}^n \cdot N_f^k| + \frac{c_{i,f}^n}{\varepsilon^2} \right) \frac{\Delta t}{\min(\Delta x_k, \Delta x_{k_f})} < Cst.$$

with the celerity of the potential wave c_i defined in section 3.1. Remark that for smooth enough solution, the right-hand-side of (2.4) is in order of $\frac{1}{2}$. In the left hand side of (2.4), the velocity of the material wave $\left|U_{i,f}^n \cdot N_f^k\right|$ is common with the CFL condition of classical Gudunov scheme. At the limit ε goes to zero, the classical CFL condition become restrictive since the wave potential is still large $c_i = O_{\varepsilon \rightarrow 0}(1)$. On the contrary, we will see in section 3.2 that the main term of the potential is constant in space, i.e. $\phi_{i,k}^n = \phi_{i,k_f}^n + O_{\varepsilon \rightarrow 0}(\varepsilon^2)$. It leads that the time step satisfying the CFL-like condition of the CPR scheme can be large, i.e. $\Delta t = O_{\varepsilon \rightarrow 0}(1)$ when ε goes to zero.

2.1. Stability and entropy dissipation. In the current section, we present a stability result based on the dissipation of the discrete mechanical energy, which act for mathematical entropy. Let us introduce the discrete kinetic energy $\mathcal{K}_k^n := \sum_{i=1}^L \mathcal{K}_{i,k}^n$ with $\mathcal{K}_{i,k}^n := \frac{\rho_i}{2} \rho_{i,k}^n \left\|U_{i,k}^n\right\|^2$ and the discrete potential energy $\mathcal{E}_k^n := \mathcal{E}(\rho_k^n)$. Eventually, the discrete mechanical energy reads $E_k^n := \mathcal{E}_k^n + \mathcal{K}_k^n$. We highlight the following result.

THEOREM 2.2 (Dissipation of the discrete mechanical energy). *Assume that the CFL-like condition (hypothesis 2.1) is fulfilled. Then for any regularization coefficient $\gamma \geq 1$, the discrete mechanical energy satisfies the following local entropy inequality (discrete version of (1.1))*

$$(2.6) \quad E_k^{n+1} \leq E_k^n - \frac{\Delta t}{\Delta x_k} \sum_{f \in \mathbb{F}_k} \sum_{i=1}^L \left(\left(\mathcal{G}_{\mathcal{K},i,f}^{n+1} + \frac{\mathcal{G}_{\mathcal{E},i,f}^{n+1}}{\varepsilon^2} \right) \cdot N_f^k + \mathcal{H}_{\mathcal{K},i,f}^{n+1} + \frac{\mathcal{H}_{\mathcal{E},i,f}^{n+1}}{\varepsilon^2} \right) \mu_f^k$$

where the flux $\mathcal{G}_{\mathcal{K},i,f}^{n+1}$, the regularization flux $\mathcal{H}_{\mathcal{K},i,f}^{n+1}$ of kinetic energy are defined by

$$(2.7) \quad \begin{aligned} \mathcal{G}_{\mathcal{K},i,f}^{n+1} \cdot N_f^k &:= \frac{1}{2} \left\|U_{i,k}^n\right\|^2 \left(\mathcal{F}_{i,f}^{n+1} \cdot N_f^k\right)^+ - \frac{1}{2} \left\|U_{i,k_f}^n\right\|^2 \left(\mathcal{F}_{i,f}^{n+1} \cdot N_f^k\right)^- \\ \mathcal{H}_{\mathcal{K},i,f}^{n+1} &:= \frac{\Delta t}{2} \left(\frac{\rho_{i,k_f}^{n+1}}{\Delta x_{k_f}} - \frac{\rho_{i,k}^{n+1}}{\Delta x_k} \right) \left\| \frac{\delta \phi_{i,f}^{n+1}}{\varepsilon^2} \right\|^2 \end{aligned}$$

the flux $\mathcal{G}_{\mathcal{E},i,f}^{n+1}$ and the regularization flux $\mathcal{H}_{\mathcal{E},i,f}^{n+1}$ of potential energy are defined by

$$(2.8) \quad \begin{aligned} \mathcal{G}_{\mathcal{E},i,f}^{n+1} \cdot N_f^k &:= \phi_{i,f}^{n+1} \mathcal{F}_{i,f}^{n+1} \cdot N_f^k \\ \mathcal{H}_{\mathcal{E},i,f}^{n+1} &:= \frac{\rho_{i,k}^{n+1} U_{i,k}^n - \rho_{i,k_f}^{n+1} U_{i,k_f}^n}{2} \cdot \delta \phi_{i,f}^{n+1}. \end{aligned}$$

Note the estimation (2.6) is a dissipation law since the terms $\mathcal{G}_{\mathcal{K},i,f}^{n+1} \cdot N_f^k$, $\mathcal{G}_{\mathcal{E},i,f}^{n+1} \cdot N_f^k$, $\mathcal{H}_{\mathcal{K},i,f}^{n+1}$ and $\mathcal{H}_{\mathcal{E},i,f}^{n+1}$ are anti-symmetric with respect to the control volume. More precisely, summing inequality (2.6) over the cell $k \in \mathbb{T}$ leads to the decreasing estimation of the global energy, which can be considered as a non-linear stability argument. For readability reasons, we start the demonstration of theorem 2.2 by two lemmas of a priori estimation of the kinetic and potential energy evolution.

LEMMA 2.3 (Kinetic energy scheme). *Assume that the CFL-like condition (Hypothesis 2.1) is fulfilled. Then the discrete kinetic energy satisfies the following esti-*

mation

$$(2.9) \quad \mathcal{K}_{i,k}^{n+1} \leq \mathcal{K}_{i,k}^n - \frac{\Delta t}{\Delta x_k} \sum_{f \in \mathbb{F}_k} \left(\mathcal{G}_{\mathcal{K},i,f}^{n+1} \cdot N_f^k + \mathcal{H}_{\mathcal{K},i,f}^{n+1} - R_{\mathcal{K},i,f}^{n+1} \right) \mu_f^k - \Delta t \frac{Q_{i,k}^{n+1}}{\varepsilon^2}$$

where the flux of potential energy $\mathcal{G}_{\mathcal{K},i,f}^n$ and $\mathcal{H}_{\mathcal{K},i,f}^n$ are defined by (2.7), the source term $R_{\mathcal{K},i,f}^n$ reads

$$(2.10) \quad R_{\mathcal{K},i,f}^{n+1} := \Delta t \frac{\rho_{i,f}^{n+1}}{\Delta x_{i,f}^{n+1}} \left\| \frac{\delta \phi_{i,f}^{n+1}}{\varepsilon^2} \right\|^2$$

and the discrete work of the force is given by

$$(2.11) \quad Q_{i,k}^{n+1} := \frac{\rho_{i,k}^{n+1} U_{i,k}^n}{\Delta x_k} \cdot \sum_{f \in \mathbb{F}_k} \delta \phi_{i,f}^{n+1} \mu_f^k.$$

Proof. According to Proposition 2.1, the mass $\rho_{i,k}^{n+1}$ are positive. Then we can write the scheme satisfy by the velocity $U_{i,k}^{n+1}$ replacing the mass $\rho_{i,k}^n$ in the momentum scheme (2.2) using the mass scheme (2.1). It leads

$$(2.12) \quad \begin{aligned} U_{i,k}^{n+1} &= U_{i,k}^n + \frac{\Delta t}{\Delta x_k} \sum_{f \in \mathbb{F}_k} \frac{U_{i,kf}^n - U_{i,k}^n}{\rho_{i,k}^{n+1}} \left(\mathcal{F}_{i,f}^{n+1} \cdot N_f^k \right)^- \mu_f^k \\ &\quad - \frac{\Delta t}{\Delta x_k} \sum_{f \in \mathbb{F}_k} \frac{\delta \phi_{i,f}^{n+1}}{\varepsilon^2} \mu_f^k. \end{aligned}$$

Since we use centered-discretization of the potential at faces, we can replace the centered-value of the potential by the half-difference, i.e.

$$\sum_{f \in \mathbb{F}_k} \phi_{i,f}^{n+1} N_f^k \mu_f^k = \sum_{f \in \mathbb{F}_k} \frac{\phi_{i,kf}^{n+1} + \phi_{i,k}^{n+1}}{2} N_f^k \mu_f^k = \sum_{f \in \mathbb{F}_k} \frac{\phi_{i,kf}^{n+1} - \phi_{i,k}^{n+1}}{2} N_f^k \mu_f^k = \sum_{f \in \mathbb{F}_k} \delta \phi_{i,f}^{n+1} \mu_f^k.$$

The scalar product between the velocity scheme (2.12) and the $\rho_{i,k}^{n+1} U_{i,k}^n$ leads to the kinetic energy scheme (2.9). Using the equality $2A \cdot (B - A) = \|B\|^2 - \|A\|^2 - \|B - A\|^2$ for any $A \in \mathbb{R}^d$ and $B \in \mathbb{R}^d$, we get

$$\mathcal{K}_{i,k}^{n+1} = \mathcal{K}_{i,k}^n - \frac{\Delta t}{\Delta x_k} \sum_{f \in \mathbb{F}_k} \left(\mathcal{G}_{\mathcal{K},i,f}^{n+1} \cdot N_f^k \right) \mu_f^k - \Delta t \frac{Q_{i,k}^{n+1}}{\varepsilon^2} + S_{i,k}^{n+1}$$

where the flux of potential energy $\mathcal{G}_{\mathcal{K},i,f}^n$ is defined by (2.7), the work of the conservative forces $Q_{i,k}^n$ is given by (2.11) and the source term $S_{i,k}^{n+1}$ coming from the numerical discretization is given by

$$S_{i,k}^{n+1} := \frac{1}{2} \rho_{i,k}^{n+1} \left\| U_{i,k}^{n+1} - U_{i,k}^n \right\|^2 - \frac{\Delta t}{\Delta x_k} \sum_{f \in \mathbb{F}_k} \frac{1}{2} \left\| U_{i,kf}^n - U_{i,k}^n \right\|^2 \left(\mathcal{F}_{i,f}^{n+1} \cdot N_f^k \right)^- \mu_f^k.$$

Let now estimate the source term $S_{i,k}^{n+1}$. Using the velocity scheme (2.12) and the Jensen's inequality, we split the advection term and the variation of potential. More

precisely we write

$$\begin{aligned} \mathcal{S}_{i,k}^{n+1} &\leq \rho_{i,k}^{n+1} \left(\frac{\Delta t}{\Delta x_k} \right)^2 \sum_{f \in \mathbb{F}_k} \left\| \frac{\delta \phi_{i,f}^{n+1}}{\varepsilon^2} \right\|^2 \mu_f^k \\ &+ \frac{1}{\rho_{i,k}^{n+1}} \left(\frac{\Delta t}{\Delta x_k} \right)^2 \left\| \sum_{f \in \mathbb{F}_k} \left(\sqrt{(\mathcal{F}_{i,f}^{n+1} \cdot N_f^k)^-} \right) \left((U_{i,k_f}^n - U_{i,k}^n) \sqrt{(\mathcal{F}_{i,f}^{n+1} \cdot N_f^k)^-} \right) \mu_f^k \right\|^2 \\ &- \frac{1}{2} \frac{\Delta t}{\Delta x_k} \sum_{f \in \mathbb{F}_k} \left\| U_{i,k_f}^n - U_{i,k}^n \right\|^2 \left(\mathcal{F}_{i,f}^{n+1} \cdot N_f^k \right)^- \mu_f^k. \end{aligned}$$

Then we slit the first term of the right-hand-side into an anti-symmetric term which leads to the flux $\mathcal{H}_{\mathcal{K},i,f}^{n+1}$ given by (2.7) and the symmetric part which leads to a source $R_{\mathcal{K},i,f}$ estimated at the faces (2.10). Eventually, using a Cauchy-Schwarz's inequality, we write the last terms of the right-hand-side and we get

$$\begin{aligned} \mathcal{S}_{i,k}^{n+1} &\leq \frac{\Delta t}{\Delta x_k} \sum_{f \in \mathbb{F}_k} \left(R_{\mathcal{K},i,f}^{n+1} - \mathcal{H}_{\mathcal{K},i,f}^{n+1} \right) \mu_f^k \\ &+ \left(\frac{\Delta t}{\Delta x_k} \sum_{f \in \mathbb{F}_k} \left\| U_{i,k_f}^n - U_{i,k}^n \right\|^2 \left(\mathcal{F}_{i,f}^{n+1} \cdot N_f^k \right)^- \mu_f^k \right) \left(\frac{\Delta t}{\Delta x_k} \sum_{f \in \mathbb{F}_k} \frac{\left(\mathcal{F}_{i,f}^{n+1} \cdot N_f^k \right)^-}{\rho_{i,k}^{n+1}} \mu_f^k - \frac{1}{2} \right). \end{aligned}$$

We conclude since under the CFL-like condition (Hypothesis 2.1), the second term of the right hand side is negative, see Proposition 2.1. \square

LEMMA 2.4 (Potential energy scheme). *The discrete potential energy satisfies the following law*

$$(2.13) \quad \mathcal{E}_k^{n+1} \leq \mathcal{E}_k^n - \frac{\Delta t}{\Delta x_k} \sum_{f \in \mathbb{F}_k} \sum_{i=1}^L \left(\mathcal{G}_{\mathcal{E},i,f}^{n+1} \cdot N_f^k + \mathcal{H}_{\mathcal{E},i,f}^{n+1} - R_{\mathcal{E},i,f}^{n+1} \right) \mu_f^k + \Delta t \sum_{i=1}^L Q_{i,k}^{n+1}$$

where the flux of potential energy $\mathcal{G}_{\mathcal{E},i,f}^n$ and $\mathcal{H}_{\mathcal{E},i,f}^n$ are defined by (2.8) and the work of the force $Q_{i,k}^n$ is given by (2.11). The numerical source term of potential energy $R_{\mathcal{E},i,f}^{n+1}$ coming from the space discretization is defined by

$$(2.14) \quad R_{\mathcal{E},i,f}^{n+1} := \left(\mathcal{F}_{i,f}^{n+1} - \rho_{i,f}^{n+1} U_{i,f}^n \right) \cdot \delta \phi_{i,f}^{n+1}$$

Proof. We introduce the potential energy at the intermediate time step $\mathcal{E}_k^{n+s} = \mathcal{E} \left(s \rho_k^{n+1} + (1-s) \rho_k^n, X_k \right)$. Using a Taylor expansion between time iteration n and $n+1$, we show that there exists $0 < s_k^* < 1$ such that

$$\begin{aligned} \mathcal{E}_k^{n+1} &= \mathcal{E}_k^n + \partial_s \mathcal{E}_k^{n+1} - \frac{1}{2} \partial_{ss}^2 \mathcal{E}_k^{n+s_k^*} \\ &= \mathcal{E}_k^n + \sum_{i=1}^L \left(\rho_{i,k}^{n+1} - \rho_{i,k}^n \right) \phi_{i,k}^{n+1} - \frac{1}{2} \sum_{i=1}^L \sum_{j=1}^L \left(\rho_{i,k}^{n+1} - \rho_{i,k}^n \right) \mathbf{H}_{ij,k}^{n+s_k^*} \left(\rho_{j,k}^{n+1} - \rho_{j,k}^n \right) \end{aligned}$$

with $\mathbf{H}_{ij,k}^{n+s_k^*} = \mathbf{H}_{ij} \left(s_k^* \rho_k^{n+1} + (1-s_k^*) \rho_k^n, X_k \right)$. Under the hypothesis 1.1, the last term is non-negative. Then, using the mass scheme (2.1), we write

$$\mathcal{E}_k^{n+1} \leq \mathcal{E}_k^n - \frac{\Delta t}{\Delta x_k} \sum_{f \in \mathbb{F}_k} \sum_{i=1}^L \phi_{i,k}^{n+1} \mathcal{F}_{i,f}^{n+1} \cdot N_f^k \mu_f^k.$$

Eventually, we make appear the exchange of energy $Q_{i,k}^{n+1}$ and we split the term estimated at the faces into an anti-symmetric flux $\mathcal{G}_{\mathcal{E},i,f}^{n+1}$ and a symmetric residual $R_{\mathcal{E},i,f}^{n+1}$ to get the announced result. \square

Note the previous estimations, lemma (2.3) and lemma (2.4), are fulfilled for any scheme under the form (2.1) and (2.2), i.e. the advection term of the momentum equation is split accordingly to the numerical mass flux. More precisely, they do not depend on the choice of the numerical mass flux $\mathcal{F}_{i,f}^{n+1}$. The theorem 2.2 is the application of the two previous lemmas in the case of the numerical mass flux $\mathcal{F}_{i,f}^{n+1}$ defined by (2.3).

Proof. [Theorem 2.2] The definition of the numerical mass flux (2.3) is motivated by the leading form of the potential energy residual (2.14). More precisely, injecting (2.3) in (2.14) and summing with (2.10), we get

$$R_{\mathcal{K},i,f}^{n+1} + \frac{R_{\mathcal{E},i,f}^{n+1}}{\varepsilon^2} = (1 - \gamma) \Delta t \frac{\rho_{i,f}^{n+1}}{\Delta x_{i,f}^{n+1}} \left\| \frac{\delta \phi_{i,f}^{n+1}}{\varepsilon^2} \right\|^2.$$

Summing the two estimations (2.9) and (2.13), we conclude the estimation of the mechanical energy (2.6) under the CFL-like condition (Hypothesis 2.1). \square

The previous estimation can be seen as an argument of global well-posedness of the CPR scheme (2.1)-(2.2)-(2.3). In particular, summing over the tessellation and the time iteration, the mechanical energy dissipation leads to the following estimation of the variation of potential at the time iteration T .

$$(\gamma - 1) \sum_{n=1}^T \Delta t \sum_{f \in \mathbb{F}} \frac{\rho_{i,f}^n}{\Delta x_{i,f}^n} \left\| \frac{\delta \phi_{i,f}^n}{\varepsilon^2} \right\|^2 \leq \sum_{k \in \mathbb{T}} \Delta x_k E_k^0$$

with \mathbb{F} the set of faces of the tessellation \mathbb{T} . However, we can not ensure that the numerical scheme can lead to a solution for any time since the sequence of time step can converge to a maximal time. In particular, in the case of there is some control volume such that the mass $\rho_{i,k}^0 = 0$, then there is no time step positive which satisfy the CFL-like condition (Hypothesis 2.1).

2.2. Consistency and accuracy order. In the current section, we study the consistency of the CPR scheme (2.1)-(2.2)-(2.3) to the conservation system of equations $M_{t,\varepsilon}$ for large parameter ε in order of 1. The proof of the consistency is established in the sense of finite difference methods, i.e. for smooth solution and on a regular cartesian grid. In the following proofs, the space step dx is the standard space step definition, i.e. the distance between the center of two neighboring cells. The normalized space step leads $\Delta x_k = \frac{|k|}{|\partial k|} = \frac{dx}{2d}$ with d the dimension. The proof is in multi-dimensional framework. However, for readability reason, we perform the space expansion in only one direction $k \in \mathbb{Z}$, with the neighbors $k - 1$ and $k + 1$ and $k + 1/2$ the face between the volume k and $k + 1$. We do not indicate the index of the other direction.

PROPOSITION 2.5 (Consistency). *Assume that the solution is smooth enough and the tessellation is a regular cartesian grid with a space step dx . Then for any regularization coefficient γ bounded with respect to Δt and dx the CPR scheme (2.1)-(2.2)-(2.3) is consistent with the conservation system of equations $M_{t,\varepsilon}$. More precisely*

the truncation error of the mass conservation (2.1) and the momentum balanced (2.2) are respectively

$$\begin{aligned} \left\| \rho_{i,k}^{n+1} - \rho_i(t^{n+1}, X_k) \right\| &= O(\Delta t, dx^2) \\ \text{and } \left\| \rho_{i,k}^{n+1} U_{i,k}^{n+1} - \rho_i(t^{n+1}, X_k) U_i(t^{n+1}, X_k) \right\| &= O(\Delta t, dx) \end{aligned}$$

assuming that the previous estimation is exact, i.e.

$$\left\| \rho_{i,k}^n - \rho_i(t^n, X_k) \right\| = \left\| \rho_{i,k}^n U_{i,k}^n - \rho_i(t^n, X_k) U_i(t^n, X_k) \right\| = 0.$$

Proof. Let us focus firstly on the mass conservation (2.1). We denote by $\rho_i|_k^n := \rho_i(t^n, X_k)$ and $U_i|_k^n := U_i(t^n, X_k)$ the exact solution of $M_{t,\varepsilon}$ at time t^n and at the position X_k . The centered scheme leads to

$$\begin{aligned} (2.15) \quad & \left(\rho_i|_{k+1}^{n+1} + \rho_i|_k^{n+1} \right) \left(\phi_i|_{k+1}^{n+1} - \phi_i|_k^{n+1} \right) - \left(\rho_i|_k^{n+1} + \rho_i|_{k-1}^{n+1} \right) \left(\phi_i|_k^{n+1} - \phi_i|_{k-1}^{n+1} \right) \\ &= 2 dx^2 \partial_x (\rho_i \partial_x \phi_i)|_k^{n+1} + O(dx^4) \\ &= 2 dx^2 \partial_x (\rho_i \partial_x \phi_i)|_k^n + O(\Delta t dx^2, dx^4) \\ \text{and } & \rho_i|_{k+1}^{n+1} U_i|_{k+1}^n - \rho_i|_{k-1}^{n+1} U_i|_{k-1}^n = 2 dx \partial_x \left(\rho_i|_k^{n+1} U_i|_k^n \right) + O(dx^3) \\ &= 2 dx \partial_x (\rho_i U_i)|_k^n + O(\Delta t dx, dx^3). \end{aligned}$$

Then we estimate the truncation error of the numerical mass flux estimated with the exact solution. More precisely, setting

$$\mathcal{F}_i|_{k+\frac{1}{2}}^{n+1} := \frac{\rho_i|_{k+1}^{n+1} U_i|_{k+1}^n + \rho_i|_k^{n+1} U_i|_k^n}{2} - \frac{d\gamma \Delta t}{\varepsilon^2} \frac{\rho_i|_{k+1}^{n+1} + \rho_i|_k^{n+1}}{2} \frac{\phi_i|_{k+1}^{n+1} - \phi_i|_k^{n+1}}{dx}$$

it is clear that the second term is one order in time smaller than the first term since γ is bounded. More precisely, using the previous estimate, we get

$$\mathcal{F}_i|_{k+\frac{1}{2}}^{n+1} - \mathcal{F}_i|_{k-\frac{1}{2}}^{n+1} = dx \partial_x (\rho_i U_i)|_k^n + O(\Delta t dx, dx^3).$$

We conclude the first truncation error using (2.1). We easily conclude for the truncation error of the momentum balanced (2.2) since the strategy is a classical upwind scheme with a centered estimation of the non-conservative term. \square

2.3. Conservation law and steady states at rest. The following section is devoted to the translation of the physical properties (1.2) and (1.3) of the model $M_{t,\varepsilon}$ to the discrete level.

PROPOSITION 2.6 (Discrete conservation of the global mass). *The discrete global mass is conserved by the CPR scheme (2.1)-(2.2)-(2.3). More precisely we have*

$$\sum_{k \in \mathbb{T}} \Delta x_k \rho_{i,k}^n = \sum_{k \in \mathbb{T}} \Delta x_k \rho_{i,k}^0.$$

Proof. The result is obvious since the numerical mass flux $\mathcal{F}_{i,f}^n$ is symmetric. \square

PROPOSITION 2.7 (Discrete conservation of the global total momentum). *Assume that the potential energy satisfies the hypothesis 1.2. Then the discrete total*

momentum is conserved by the CPR scheme (2.1)-(2.2)-(2.3). More precisely we have

$$\begin{aligned} \sum_{i=1}^L \rho_{i,k}^{n+1} U_{i,k}^{n+1} &= \sum_{i=1}^L \rho_{i,k}^n U_{i,k}^n - \frac{\Delta t}{\Delta x_k} \sum_{f \in \mathbb{F}_k} \sum_{i=1}^L \frac{\rho_{i,k}^{n+1} \phi_{i,k_f}^{n+1} + \rho_{i,k_f}^{n+1} \phi_{i,k}^{n+1}}{4\varepsilon^2} \mu_f^k \\ &\quad - \frac{\Delta t}{\Delta x_k} \sum_{f \in \mathbb{F}_k} \sum_{i=1}^L \left(U_{i,k}^n \left(\mathcal{F}_{i,f}^{n+1} \cdot N_f^k \right)^+ - U_{i,k_f}^n \left(\mathcal{F}_{i,f}^{n+1} \cdot N_f^k \right)^- \right) \mu_f^k. \end{aligned}$$

Proof. We focus on the non-conservative term of (2.2). At the discrete level, the hypothesis 1.2 leads to write $\phi_{i,k}^{n+1} = \sum_{j=1}^L \mathbf{H}_{ij} \rho_{j,k}^{n+1}$ with the hessian symmetric, i.e. $\mathbf{H}_{ij} = \mathbf{H}_{ji}$. Summing the momentum scheme (2.2) over the mass $1 \leq i \leq L$, the non-conservative term becomes

$$\sum_{i=1}^L \rho_{i,k}^{n+1} \sum_{f \in \mathbb{F}_k} \frac{\phi_{i,f}^{n+1}}{\varepsilon^2} N_f^k \mu_f^k = \sum_{f \in \mathbb{F}_k} \sum_{i=1}^L \frac{\rho_{i,k}^{n+1} \phi_{i,k_f}^{n+1}}{2\varepsilon^2} N_f^k \mu_f^k = \sum_{f \in \mathbb{F}_k} \sum_{i=1}^L \sum_{j=1}^L \frac{\rho_{i,k}^{n+1} \mathbf{H}_{ij} \rho_{j,k_f}^{n+1}}{2\varepsilon^2} N_f^k \mu_f^k.$$

Since the hessian is symmetric, i.e. $\mathbf{H}_{ij} = \mathbf{H}_{ji}$, we write

$$\sum_{i=1}^L \rho_{i,k}^{n+1} \sum_{f \in \mathbb{F}_k} \frac{\phi_{i,f}^{n+1}}{\varepsilon^2} N_f^k \mu_f^k = \sum_{f \in \mathbb{F}_k} \sum_{i=1}^L \sum_{j=1}^L \frac{\rho_{j,k_f}^{n+1} \mathbf{H}_{ji} \rho_{i,k}^{n+1}}{2\varepsilon^2} N_f^k \mu_f^k = \sum_{f \in \mathbb{F}_k} \sum_{j=1}^L \frac{\rho_{j,k}^{n+1} \phi_{j,k_f}^{n+1}}{2\varepsilon^2} N_f^k \mu_f^k.$$

We conclude summing the second and the last expressions. \square

PROPOSITION 2.8 (Well-balanced). *The CPR scheme (2.1)-(2.2)-(2.3) preserves the steady states at rest defined by $U_{i,k}^n = 0$ and $\phi_{i,k}^n = \bar{\phi}_i$.*

Proof. Assume that the scheme satisfies the steady state at time iteration n . Let us consider first the mass scheme (2.1). Since the velocity and the variation of potential vanish $U_{i,f}^n = 0$ and $\delta\phi_{i,f}^n = 0$, the scheme can be written as

$$\rho_{i,k}^{n+1} - \gamma \frac{\Delta t^2}{\Delta x_k} \sum_{f \in \mathbb{F}_k} \rho_{i,f}^{n+1} \frac{\delta\phi_{i,f}^{n+1}}{\varepsilon^2 \Delta x_{i,f}^{n+1}} \cdot N_f^k \mu_f^k = \rho_{i,k}^n - \gamma \frac{\Delta t^2}{\Delta x_k} \sum_{f \in \mathbb{F}_k} \rho_{i,f}^n \frac{\delta\phi_{i,f}^n}{\varepsilon^2 \Delta x_{i,f}^n} \cdot N_f^k \mu_f^k.$$

Then the unique solution is the steady solution $\rho_{i,k}^{n+1} = \rho_{i,k}^n$, which implies $\phi_{i,k}^{n+1} = \phi_i(\rho_k^{n+1}, X_k) = \phi_i(\rho_k^n, X_k) = \bar{\phi}_i$. Eventually, the velocity at time iteration $n+1$ vanishes $U_{i,f}^{n+1} = 0$ since the numerical flux $\mathcal{F}_{i,f}^{n+1}$ and the potential variation $\delta\phi_{i,f}^{n+1}$ term vanish. \square

3. Asymptotic regimes. In the following section, we detail the behavior of the scheme in the regime $\varepsilon \ll 1$. The advection model $M_{t,\varepsilon}$ has two relevant asymptotic behaviors in function of the time scale considered. For small enough time, the smooth solutions of model $M_{t,\varepsilon}$ are close to the system of a coupled system of wave equations $M_{\tau,0}$. For large enough time scale, the model $M_{t,\varepsilon}$ tends to the solution of the divergence free model $M_{t,0}$. For each time scale, we present a formal derivation of the continuous asymptotic model. Then we identify the numerical scheme at the limit ε goes to zero and we study the consistency of the asymptotic scheme to the asymptotic model.

3.1. Fine time scale: the wave equations $M_{\tau,0}$. In the following section, we are interested into the behavior of the solution of $M_{t,\varepsilon}$ for a small time scale $t = \varepsilon\tau$ and at the limit ε goes to zero. Assuming the solution smooth enough, we consider the time derivative of the mass conservation and the space derivative of the momentum balance. It leads

$$(M_{\tau,\varepsilon}) \quad \left\{ \partial_{\tau\tau}^2 \rho_i - \nabla \cdot (\varepsilon^2 \nabla \cdot (\rho_i U_i \otimes U_i) + \rho_i \nabla \phi_i) \right\} = 0.$$

Assuming that the velocity U_i is independently bounded with respect to ε , we formally get the model $M_{\tau,0}$ at the limit ε goes to zero. In addition, the error between the two models is in order of ε^2 , for well-prepared initial condition. Remark that considering the momentum equation, the gradient of the potential has to be small enough $\nabla \phi_i = O_{\varepsilon \rightarrow 0}(\varepsilon)$ to make the velocity U_i bounded in ε . In particular at the initial condition, the derivation required

$$(3.1) \quad \nabla \phi_i(\rho^0) = O_{\varepsilon \rightarrow 0}(\varepsilon) \quad \text{and} \quad U_i^0 = O_{\varepsilon \rightarrow 0}(1).$$

For more details about the derivation and analytical result on the wave equations, we refer to [43]. Note that the model $M_{\tau,0}$ can be written as

$$\partial_{\tau\tau}^2 \tilde{\rho}_i - \sum_{j=1}^L \nabla \cdot \left(\tilde{\rho}_i \tilde{\mathbf{H}}_{ij} \nabla \tilde{\rho}_j \right) = \nabla \cdot \left(\tilde{\rho}_i \left(\nabla \tilde{\phi}_i \right)_{\tilde{\rho}} \right)$$

with $\left(\nabla \tilde{\phi}_i \right)_{\tilde{\rho}}$ is the space derivative of $\tilde{\phi}_i(\tilde{\rho}, X)$ for a fixed vector $\tilde{\rho}$. Since the hessian $\tilde{\mathbf{H}} = \mathbf{H}(\tilde{\rho}, X)$ is positive-definite, the matrix $\tilde{\rho}_i \tilde{\mathbf{H}}_{ij}$ is definite-positive. It leads that the system of wave equations $M_{\tau,0}$ is hyperbolic, at least in the case of the space variation of the potential can be neglected when ε goes to zero, i.e. $(\nabla \phi_i)_{\rho} = O_{\varepsilon \rightarrow 0}(\varepsilon)$. More precisely, we define the wave speeds $(c_i)_{1 \leq i \leq L}$ such that the square of the wave speeds are the eigenvalues of the matrix $\tilde{\rho}_i \tilde{\mathbf{H}}_{ij}$. Then the solution of the wave equations $M_{\tau,0}$ with $\left(\nabla \tilde{\phi}_i \right)_{\tilde{\rho}} = 0$ is given by the Kirchoff's formulae.

Let us now consider the following scheme

$$(3.2) \quad \frac{\tilde{\rho}_{i,k}^{n+1} - 2\tilde{\rho}_{i,k}^n + \tilde{\rho}_{i,k}^{n-1}}{\Delta\tau^2} = \frac{1}{2\Delta x_k} \sum_{f \in \mathbb{F}_k} \left(\frac{\tilde{\rho}_{i,k_f}^n}{\Delta x_{k_f}} \sum_{g \in \mathbb{F}_{k_f}} \tilde{\phi}_{i,g}^n N_g^{k_f} \mu_g^{k_f} \right) \cdot N_f^k \mu_f^k \\ + \frac{\gamma}{\Delta x_k} \sum_{f \in \mathbb{F}_k} \left(\tilde{\rho}_{i,f}^{n+1} \frac{\delta \tilde{\phi}_{i,f}^{n+1}}{\Delta x_{i,f}^{n+1}} - \tilde{\rho}_{i,f}^n \frac{\delta \tilde{\phi}_{i,f}^n}{\Delta x_{i,f}^n} \right) \cdot N_f^k \mu_f^k.$$

Obviously the numerical scheme (3.2) is not classical for the wave equations $M_{\tau,0}$ model and it is not the most efficient, in particular because of the large stencil. However, it is consistent with the wave equations $M_{\tau,0}$. More precisely, we get the following result.

PROPOSITION 3.1. *Assume that the solution is smooth enough and the tessellation is a regular cartesian grid with a space step dx . Then the numerical strategy (3.2) is consistent with the wave equations $M_{\tau,0}$. More precisely the truncation error is*

$$\left\| \tilde{\rho}_{i,k}^{n+1} - \tilde{\rho}_i(\tau^{n+1}, X_k) \right\| = O(\Delta\tau, dx^2).$$

Proof. Let us start by write the numerical scheme (3.2) on the cartesian grid using the notation introduce in Section 2.2. Note the discrete cross products between the direction vanish because of the scalar product between the normal $N_g^{k_f} \cdot N_f^k$. It leads

$$\begin{aligned} \frac{\tilde{\rho}_i|_k^{n+1} - 2\tilde{\rho}_i|_k^n + \tilde{\rho}_i|_k^{n+1}}{\Delta\tau^2} &= \frac{1}{2\,dx} \left(\tilde{\rho}_i|_{k+1}^n \frac{\tilde{\phi}_i|_{k+2}^n - \tilde{\phi}_i|_k^n}{2\,dx} - \tilde{\rho}_i|_{k-1}^n \frac{\tilde{\phi}_i|_k^n - \tilde{\phi}_i|_{k-2}^n}{2\,dx} \right) \\ &+ \frac{d\gamma}{dx} \left(\frac{\tilde{\rho}_i|_k^{n+1} + \tilde{\rho}_i|_{k+1}^{n+1}}{2} \frac{\tilde{\phi}_i|_{k+1}^{n+1} - \tilde{\phi}_i|_k^{n+1}}{dx} - \frac{\tilde{\rho}_i|_k^{n+1} + \tilde{\rho}_i|_{k-1}^{n+1}}{2} \frac{\tilde{\phi}_i|_k^{n+1} - \tilde{\phi}_i|_{k-1}^{n+1}}{dx} \right) \\ &- \frac{d\gamma}{dx} \left(\frac{\tilde{\rho}_i|_k^n + \tilde{\rho}_i|_{k+1}^n}{2} \frac{\tilde{\phi}_i|_{k+1}^n - \tilde{\phi}_i|_k^n}{dx} - \frac{\tilde{\rho}_i|_k^n + \tilde{\rho}_i|_{k-1}^n}{2} \frac{\tilde{\phi}_i|_k^n - \tilde{\phi}_i|_{k-1}^n}{dx} \right) \end{aligned}$$

We conclude using the centered scheme truncation error. \square

PROPOSITION 3.2 (Consistency with the asymptotic model $M_{\tau,0}$). *Assume that the potential satisfies the Hypothesis 1.3 and the discretized initial condition satisfies*

$$\rho_{i,k}^0 = O_{\varepsilon \rightarrow 0}(1), \quad U_{i,k}^0 = O_{\varepsilon \rightarrow 0}(1) \quad \text{and} \quad \phi_i(\rho_k^0, X_k) = \phi_i^0 + O_{\varepsilon \rightarrow 0}(\varepsilon).$$

Then the CPR scheme (2.1)-(2.2)-(2.3) with the time step scaling $\Delta t = O_{\varepsilon \rightarrow 0}(\varepsilon)$ tends to the scheme (3.2) at the limit ε goes to zero. More precisely we have for any time iteration $n \in \mathbb{N}$, any control volume $k \in \mathbb{T}$

$$|\rho_{i,k}^n - \tilde{\rho}_{i,k}^n| = O_{\varepsilon \rightarrow 0}(\varepsilon^2)$$

with $\rho_{i,k}^n$ solution of the CPR scheme (2.1)-(2.2)-(2.3) and $\tilde{\rho}_{i,k}^n$ solution of the scheme (3.2).

Proof. Assume that the variation of potential at time iteration n is small enough, i.e. $\phi_{i,k}^n = \phi_i^n + O_{\varepsilon \rightarrow 0}(\varepsilon)$ which is true at the initial condition. The main term of the mass scheme (2.1) can be written as

$$\rho_{i,k}^{n+1} - \gamma \frac{\Delta\tau^2}{\Delta x_k} \sum_{f \in \mathbb{F}_k} \rho_{i,f}^{n+1} \frac{\delta\phi_{i,f}^{n+1}}{\Delta x_{i,f}^{n+1}} \cdot N_f^k \mu_f^k = \rho_{i,k}^n - \gamma \frac{\Delta\tau^2}{\Delta x_k} \sum_{f \in \mathbb{F}_k} \rho_{i,f}^n \frac{\delta\phi_{i,f}^n}{\Delta x_{i,f}^n} \cdot N_f^k \mu_f^k + O_{\varepsilon \rightarrow 0}(\varepsilon).$$

Taking into account the regularity of the potential, see hypothesis 1.3, we get

$$\phi_i \left(\rho_k^n + O_{\varepsilon \rightarrow 0}(\varepsilon), X_k \right) = \phi_i(\rho_k^n, X_k) + \sum_{j=1}^L (\mathbf{H}_{ij})_k^n O_{\varepsilon \rightarrow 0}(\varepsilon) = \phi_i^n + O_{\varepsilon \rightarrow 0}(\kappa\varepsilon)$$

with $(\mathbf{H}_{ij})_k^n = \mathbf{H}_{ij}(\rho_k^n, X_k)$. Then the solution for the main term is $\rho_{i,k}^{n+1} = \rho_{i,k}^n + O_{\varepsilon \rightarrow 0}(\varepsilon)$. We conclude by induction that the main term of the mass is a constant in time, then the main term of the potential is a constant in time and in space. Then the variation of potential $\delta\phi_{i,f}^{n+1}$ is in order of ε and the numerical mass flux $\mathcal{F}_{i,k}^n$ is

in order of 1. Simplified by the main term of the mass, the momentum scheme (2.2) leads

$$U_{i,k}^{n+1} = U_{i,k}^n - \frac{\Delta\tau}{\Delta x_k} \sum_{f \in \mathbb{F}_k} \frac{\delta\phi_{i,f}^{n+1}}{\varepsilon} \mu_f^k + O_{\varepsilon \rightarrow 0}(\varepsilon).$$

Eventually, considering the difference between two time steps of the mass scheme (2.1) and injecting the main term of the velocity into the mass scheme, we get the numerical scheme (3.2) with a second order perturbation. \square

3.2. Large time scale: the divergence free model $M_{t,0}$. The following section is devoted to the study of the behavior of the solution of $M_{t,\varepsilon}$ at the limit ε goes to zero and for a large enough time scale, i.e. $t = O_{\varepsilon \rightarrow 0}(1)$. This regime, so-called low-Mach number regime for gas dynamic or low-Froude number regime for free surface flow, is relevant for many applications such are nuclear reactor [7] and oceanography [37]. At the limit ε goes to zero, the main term of the momentum equation of $M_{t,\varepsilon}$ formally reads $\nabla\phi_i = O_{\varepsilon \rightarrow 0}(\varepsilon^2)$. Let us now consider the scalar product between the time derivative of the potential and of the mass, i.e.

$$\partial_t\phi \cdot \partial_t\rho = \partial_t\phi \cdot \mathbf{H}^{-1}\partial_t\phi \geq 0$$

After integration over the space domain and using the mass conservation, we conclude that the left hand side is in order of ε^2 . Since the right hand side is non-negative, we conclude that, except in a domain of measure in order of ε , the time derivative of the potential is almost everywhere in order of ε^2 . Formally we get $\partial_t\phi = O_{\varepsilon \rightarrow 0}(\varepsilon^2)$. Composing the mass conservation by the hessian, we get the divergence free constrain $\nabla \cdot (\rho_i U_i) = O_{\varepsilon \rightarrow 0}(\varepsilon^2)$. Then since the condition number is small enough with respect to the small parameter ε , see Hypothesis 1.3, we conclude that the main term of the potential is constant in time and space. The main term of the mass corresponds to the average value the potential at the initial condition, i.e.

$$\phi_i(\bar{\rho}) = \frac{1}{|\Omega|} \int_{\Omega} \phi_i(\rho^0) \, dX$$

and we formally get the divergence free constrain of the model $M_{t,0}$. The second equation of the divergence free model $M_{t,0}$ is given by the equation of the velocity, so-called non-conservative form of the momentum equation of $M_{t,\varepsilon}$, taking into account the space variation of the potential is in order of ε^2 . Note to give a sense to the derivation, the initial condition has to be well-prepared, i.e. the initial condition of the mass should satisfies the scaling $\nabla\phi_i(\rho^0) = O_{\varepsilon \rightarrow 0}(\varepsilon^2)$ and $\nabla \cdot (\rho_i^0 U_i^0) = O_{\varepsilon \rightarrow 0}(\varepsilon^2)$. The non well-prepared initial conditions lead to the formation of a so-called initial layer, see [20, 21, 22]. In addition, in the case with the space variation of the potential is small enough, i.e. $(\nabla\phi_i)_\rho = O_{\varepsilon \rightarrow 0}(\varepsilon)$, the mass is constant in space and it has play in the velocity dynamics. More precisely, it can be simplified from the divergence free constrain in $M_{t,0}$. It leads the classical incompressible Euler model in the context of gas dynamic. Except for the estimation of the parameters $\bar{\rho}_i$, the divergence free model $M_{t,0}$ is composed by L systems which are not coupled.

Let us now consider the following scheme

$$(3.3) \quad \begin{aligned} \bar{U}_{i,k}^{n+1} &= \bar{U}_{i,k}^n - \frac{\Delta t}{\Delta x_k} \sum_{f \in \mathbb{F}_k} \delta \bar{\phi}_{i,f}^{n+1} \mu_f^k \\ &\quad - \frac{\Delta t}{\bar{\rho}_{i,k} \Delta x_k} \sum_{f \in \mathbb{F}_k} \left(\bar{U}_{i,k}^n \left(\bar{\mathcal{F}}_{i,f}^{n+1} \cdot N_f^k \right)^+ - \bar{U}_{i,k_f}^n \left(\bar{\mathcal{F}}_{i,f}^{n+1} \cdot N_f^k \right)^- \right) \mu_f^k \end{aligned}$$

with the parameters $\bar{\rho}_{i,k} > 0$, $2\bar{\rho}_{i,f} := \bar{\rho}_{i,k} + \bar{\rho}_{i,k_f}$, $2\frac{\bar{\rho}_{i,f}}{\Delta x_{i,f}} := \frac{\bar{\rho}_{i,k}}{\Delta x_k} + \frac{\bar{\rho}_{i,k_f}}{\Delta x_{k_f}}$ and the asymptotic mass flux $\bar{\mathcal{F}}_{i,f}^{n+1} := \bar{\rho}_{i,f} \left(\bar{U}_{i,f}^n - \gamma \Delta t \frac{\delta \bar{\phi}_{i,f}^{n+1}}{\Delta x_{i,f}} \right)$. The variation of the perturbation of the potential $\delta \bar{\phi}_{i,f}^{n+1}$ is given by

$$(3.4) \quad \sum_{f \in \mathbb{F}_k} \bar{\mathcal{F}}_{i,f}^{n+1} \mu_f^k = \sum_{f \in \mathbb{F}_k} \bar{\rho}_{i,f} \left(\bar{U}_{i,f}^n - \gamma \Delta t \frac{\delta \bar{\phi}_{i,f}^{n+1}}{\Delta x_{i,f}} \right) \cdot N_f^k \mu_f^k = 0.$$

The numerical scheme (3.3) can be classified to the pseudo-compressible methods with a relaxation of the constrain, see [40]. In particular, the divergence free constrain is not exactly satisfied at the discrete level. However, it is consistent with the divergence free model $M_{t,0}$. More precisely, we get the following result.

PROPOSITION 3.3. *Assume that the solution is smooth enough and the tessellation is a regular cartesian grid with a space step dx . Then the numerical strategy (3.3) is consistent with the divergence free model $M_{t,0}$. More precisely the truncation error of the Lagrange multiplier and the truncation error of the velocity are respectively*

$$\begin{aligned} \left\| \bar{\phi}_{i,k}^{n+1} - \bar{\phi}_i(t^{n+1}, X_k) \right\| &= O(\Delta t, dx^2) \\ \text{and } \left\| \bar{U}_{i,k}^{n+1} - \bar{U}_i(t^{n+1}, X_k) \right\| &= O(\Delta t, dx). \end{aligned}$$

Proof. We use the notation introduce in Section 2.2. Let us start by the divergence free constrain (3.4). The centered scheme used to discretize the divergence (3.4) leads to

$$\partial_x \bar{\mathcal{F}}_i|_k^n = \partial_x (\bar{\rho}_i \bar{U}_i)|_k^n - d\gamma \Delta t \partial_x (\bar{\rho}_i \partial_x \bar{\phi}_i)|_k^{n+1} = O(dx^2)$$

with $\bar{\rho}_{i,k} = \bar{\rho}_i(X_k)$ and $\bar{U}_i(t, X)$ the solution of $M_{t,0}$. Then scheme on the velocity (3.3) is a classical upwind scheme and leads to

$$\partial_t \bar{U}_i|_k^n + \nabla \cdot (\bar{\rho}_i \bar{U}_i \otimes \bar{U}_i)|_k^n + \nabla \bar{\phi}_i|_k^n = O(\Delta t, dx)$$

Since the divergence of the mass flux vanishes, we get $\nabla \cdot (\bar{\rho}_i \bar{U}_i \otimes \bar{U}_i) = \bar{\rho}_i (\bar{U}_i \cdot \nabla) \bar{U}_i$ and we conclude. \square

PROPOSITION 3.4 (Consistency with the asymptotic model $M_{t,0}$). *Assume that the potential satisfies the Hypothesis 1.3 and the discretized initial condition satisfies*

$$\rho_{i,k}^0 = O_{\varepsilon \rightarrow 0}(1), \quad U_{i,k}^0 = O_{\varepsilon \rightarrow 0}(1) \quad \text{and} \quad \phi_i(\rho_k^0, X_k) = \phi_i^0 + O_{\varepsilon \rightarrow 0}(\varepsilon^2).$$

Then the CPR scheme (2.1)-(2.2)-(2.3) with the time step scaling $\Delta t = O_{\varepsilon \rightarrow 0}(1)$ tends to the scheme (3.3) at the limit ε goes to zero. More precisely we have for any time iteration $n \in \mathbb{N}$ and any control volume $k \in \mathbb{T}$

$$|\rho_{i,k}^n - \bar{\rho}_{i,k}| = O_{\varepsilon \rightarrow 0}(\varepsilon^2) \quad \text{and} \quad |U_{i,k}^n - \bar{U}_{i,k}^n| = O_{\varepsilon \rightarrow 0}(\varepsilon^2)$$

with $\rho_{i,k}^n$ solution of the CPR scheme (2.1)-(2.2)-(2.3) and $\bar{U}_{i,k}^n$ solution of the scheme (3.2) with $\bar{\rho}_{i,k}$ given by $\phi_i(\bar{\rho}_k, X_k) = \phi_i^0$.

Proof. Since the mass are positive (Proposition 2.1) and the numerical scheme conserves the global mass (Proposition 2.6), the mass in a control volume $\rho_{i,k}^{n+1}$ is bounded by the initial value, i.e. $\Delta x_k \rho_{i,k}^{n+1} \leq \sum_{j \in \mathbb{T}} \Delta x_j \rho_{i,j}^0 = O_{\varepsilon \rightarrow 0}(1)$. Then the main term of the mass scheme (2.1) reads

$$-\frac{\Delta t}{\Delta x_k} \sum_{f \in \mathbb{F}_k} \rho_{i,f}^{n+1} \frac{\gamma \Delta t}{\varepsilon^2} \frac{\delta \phi_{i,f}^{n+1}}{\Delta x_{i,f}^{n+1}} \cdot N_f^k \mu_f^k = O_{\varepsilon \rightarrow 0}(1).$$

We conclude that for any $f \in \mathbb{F}$, we have $\delta \phi_{i,f}^{n+1} = O_{\varepsilon \rightarrow 0}(\varepsilon^2)$, then the main term of the potential is constant in space, i.e. $\phi_{i,k}^n = \phi_i^n + O_{\varepsilon \rightarrow 0}(\varepsilon^2)$. In another hand, for any $X \in \Omega$, since the hessian \mathbf{H} is positive-definite, the application $\phi(\rho, X)$ is a diffeomorphism accordingly to the inverse function theorem. We define the mass at the intermediate time $\rho_{i,k}^{n+s} = \rho_i(s \phi_k^{n+1} + (1-s) \phi_k^n, X_k)$ with $\rho(\phi, X)$ the inverse function for a given X of $\phi(\rho, X)$. Accordingly to the mean value theorem, for any system $1 \leq i \leq L$ and any control volumes k , there exists an intermediate time $0 < s_{i,k}^* < 1$ such that

$$\rho_{i,k}^{n+1} - \rho_{i,k}^n = \sum_{j=1}^L (\mathbf{H}_{ij}^{-1})_k^{n+s_{i,k}^*} (\phi_{j,k}^{n+1} - \phi_{j,k}^n)$$

with $(\mathbf{H}_{ij}^{-1})_k^{n+s_{i,k}^*} = \mathbf{H}_{ij}^{-1}(s_{i,k}^* \rho_k^{n+1} + (1-s_{i,k}^*) \rho_k^n, X_k)$ positive-definite. After summing over the control volume, since the main term of the potential is constant in space and using the mass conservation, we get

$$\sum_{j=1}^L \mathbf{M}_{ij} (\phi_j^{n+1} - \phi_j^n) = O_{\varepsilon \rightarrow 0}(\varepsilon^2).$$

with $\mathbf{M}_{ij} = \left(\sum_{k \in \mathbb{T}} \Delta x_k (\mathbf{H}_{ij}^{-1})_k^{n+s_{i,k}^*} \right)$ positive-definite as a sum of positive-definite matrices. Likewise, \mathbf{M} is well-conditioned independently of ε , i.e. the condition number $\kappa(\mathbf{M}) = O_{\varepsilon \rightarrow 0}(1)$. We conclude that the main term of the potential is constant in space and in time, i.e. $\phi_{i,k}^{n+1} = \phi_i^0 + O_{\varepsilon \rightarrow 0}(\kappa \varepsilon^2)$. It leads that the mass is close enough to the parameter of the asymptotic scheme $\bar{\rho}_{i,k}$, i.e. $\rho_{i,k}^n = \bar{\rho}_{i,k} + O_{\varepsilon \rightarrow 0}(\kappa \varepsilon^2)$. More precisely, using the mean value theorem between the initial time and the time of the n^{th} iteration, we write

$$\rho_{i,k}^n = \rho_i(\phi_k^n, X_k) = \rho_i(\phi^0, X_k) + O_{\varepsilon \rightarrow 0}(\kappa^2 \varepsilon^2) = \bar{\rho}_{i,k} + O_{\varepsilon \rightarrow 0}(\kappa^2 \varepsilon^2).$$

Accordingly to the mean value theorem, for any system $1 \leq i \leq L$ and any control volumes k , there exists an intermediate time $0 < s_{i,k} < 1$ such that

$$\phi_{i,k}^{n+1} - \phi_{i,k}^n = \sum_{j=1}^L (\mathbf{H}_{ij})_k^{n+s_{i,k}} \left(\rho_{j,k}^{n+1} - \rho_{j,k}^n \right)$$

with $(\mathbf{H}_{ij})_k^{n+s_{i,k}} = \mathbf{H}_{ij} \left(s_{i,k} \rho_k^{n+1} + (1 - s_{i,k}) \rho_k^n, X_k \right)$. Using the mass conservation (2.1) we get the divergence free condition (3.4) with a second order perturbation. In addition, replacing the mass $\rho_{i,k}^{n+1}$ by the parameter $\bar{\rho}_{i,k}$ into the momentum scheme (2.2), we get the asymptotical scheme on the velocity (3.3) with a second order perturbation. Note that the asymptotic unknown $\bar{\phi}_{i,k}^n$ corresponds to the second perturbation with respect to ε of the potential $\phi_{i,k}^n$. More precisely, we have the estimation $\phi_{i,k}^n = \phi_i^0 + \varepsilon^2 \bar{\phi}_{i,k}^n + O(\varepsilon^4)$ and then $\rho_{i,k}^n = \bar{\rho}_{i,k} + \varepsilon^2 \rho_i \left(\bar{\phi}_{i,k}^n, X_k \right) + O(\varepsilon^4)$. \square

4. Numerical results. The current section is devoted to the illustration of the analytical results obtained in section 2 and 3. The following simulations are presented in the framework of free surface flow in 1 space dimension. More precisely, the unknowns are $\rho_i(t, x) = \varrho_i h_i(t, x)$ with ϱ_i are the density of the fluid in the i^{th} layer, numbered from the free surface to the bottom. In order to satisfy hypothesis 1.1, the density is increasing in the following, i.e. $\varrho_1 < \varrho_2 < \dots < \varrho_N$. The potential ϕ_i is given by the physical pressure in the layer. More precisely, we have $\phi_i = g \left(z_b + \sum_{j=1}^L \frac{\varrho_j h_j}{\varrho_{\max(i,j)}} \right)$, with $z_b(x)$ the bottom elevation and the gravity acceleration g is set to 9.81.

4.1. Lake at rest. The steady state at rest proposition 2.8 in the framework of free surface flow is the so-called lake at rest and can be written as

$$\forall 1 \leq i < N, \quad h_{i,k}^n = Cst \quad \text{and} \quad h_{L,k}^n + z_b = Cst.$$

We perform several numerical simulations with various bottom elevation, continuous or not, with several layers and small or large density variations to validate the numerical conservation of the steady state of the lake at rest. The proposition is satisfied in any situations while the bottom elevation is completely immersed, i.e. $h_{L,k}^n > 0$ and the density is increasing, with the error of the resolution method of the linear system. Note that due to the CFL condition (2.4), the dry areas can not be simulated by the CPR method proposed in the current paper. More precisely, the CFL condition (2.4) with dry area leads to a vanishing time step.

4.2. Simulation of oscillating surfaces.

This test case is the simulation of oscillating layers around the steady state at rest in an infinite domain. More precisely the initial condition is given by

$$h_1^0(x) = 10^3 + \cos(2\pi x), \quad \forall 2 \leq i \leq L = 5 \quad h_i^0(x) = 10^3$$

and $u_1^0 = u_2^0 = z_b = 0$. The density of the layer is given by $\varrho_i = 10 + i$. The simulation can be seen as a simplified modeling of ocean flow, neglecting several external forces such as the Coriolis force and atmospheric pressure variation. In such context, the total water depth is around $5 \cdot 10^3$ meters but the density should varie from 1020 to $1035 \text{ kg} \cdot \text{m}^{-3}$. We increase the ratio of density between the layer to present clearer results. More precisely, in the real ocean context, the wave celerities are too different to be identified with the same time scale. The analysis in the case of small variation

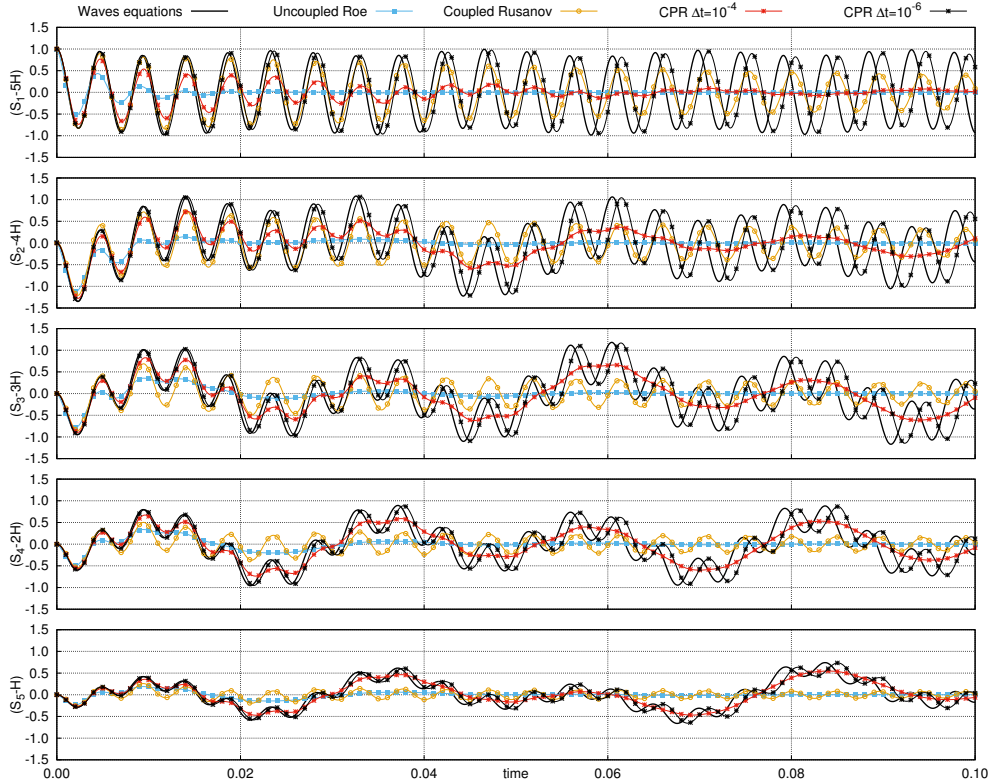


FIG. 1. *Simulation of oscillating surfaces: Comparison between the CPR scheme ($\gamma = 1$ with $\Delta t = 10^{-4}$ and $\Delta t = 10^{-6}$), the Rusanov scheme with the coupled strategy ($\Delta t = 10^{-4}$), the Roe scheme with the uncoupled strategy ($\Delta t = 10^{-4}$), and the analytical solution of the asymptotic wave equations $M_{\tau,0}$. Each row represents the deviation of the surfaces ($S_j = \sum_{i=j}^L h_i$) from the steady state of the lake at rest at the position $x = 0$ along the time.*

of density is presented in section 4.4. The objective of the current test case is to compare the CPR scheme at the low-Froude number regime to an analytical solution of the asymptotic model $M_{\tau,0}$, obtained by the D'Alembert's formulae. The eigenvalues and the eigenvectors required for the D'Alembert's formulae are determined numerically in the following using a QR decomposition with Givens rotations. The solution of the asymptotic model is a superposition of five waves. Two of them can clearly be identified in Fig. 1, one with a high frequency, close to the frequency of the monolayer shallow water, and one with a low frequency. Note that the amplitude of the oscillations of the internal layers can be larger than the amplitude of the initial perturbation because of interferences, see Fig. 1 third surface S_3 at time $t = 0.06$. We compare the numerical result with a space step $dx = 5 \cdot 10^{-2}$ obtained using the Rusanov scheme for the coupled model of shallow water equations, the Roe scheme for the uncoupled treatment [9] and the CPR scheme with two different time step ($\Delta t = 10^{-4}$ and $\Delta t = 10^{-6}$). Note that the Rusanov scheme with the coupled model and the Roe scheme with the uncoupled treatment required a time step $\Delta t = 10^{-4}$ for stability. The CPR scheme can be use with a larger time step but the result is very diffusive. Accordingly to the scaling analysis, the time step of the CPR scheme should be in order of ε to get an approximation of the wave equations $M_{\tau,0}$.

The coupled strategy (Coupled Rusanov in Fig. 1) is able to preserve the amplitude of the highest frequency, by adjusting the time step. However, the lower the frequencies are, the more diffusive the wave is. This observation is true for any coupled Godunov scheme and the smaller the time step, the larger the diffusion is. In particular the coupled strategy is not able to recover the lower frequencies for a long time simulation. Obviously, the applications in the context of oceanic flow are interesting into long time simulations, from several hours to one years, and the low-frequencies are the most representative of the flow. In the case of the uncoupled treatment (Uncoupled Roe in Fig. 1), the numerical diffusion is almost similar for all the frequencies. However, the diffusion is very large and become even larger when the time step is smaller such as the coupled strategy. On the contrary, the solution obtained with the CPR scheme is less diffusive for the lower frequencies than for the higher frequencies. More precisely, with the same time step use for the stability of the Godunov scheme, i.e. $\Delta t = 10^{-4}$, the CPR scheme well-preserve the amplitude of the lowest frequency wave. In addition, the smaller the time step is, the smaller the diffusion is for the high frequencies. Using a time step of $\Delta t = 10^{-6}$, the amplitude of the highest frequency wave is well-preserved during the time of the simulation. Note all the numerical results presented above have a phase shift. This phase shift is not corrected by the CPR scheme when the time step goes to zero. It is link to the space discretization. The smaller the space step is, the smaller the phase shift is. Eventually, we recall that the coupled Lax-Wendroff scheme leads to excellent results for this test case. It exactly preserve the amplitude of of all the frequencies but it present the same phase shift than the CPR scheme. The Lax-Wendroff solver is a second order scheme in time and space.

4.3. Dam break simulation.

This test case is the Stoker’s solution [42]. The bottom elevation is flat, i.e. $z_b = 0$, the initial water level is given by

$$h_1^0(x) = \begin{cases} 1.5 & , \text{if } x < 0.5 \\ 0.5 & , \text{elsewhere.} \end{cases}$$

and the initial velocity vanishes, i.e. $u_1^0(x) = 0$. The objective of this test case is to illustrate the robustness of the scheme for large number $\varepsilon \approx 1$. In Fig. 2, we compare the water elevation (first row) and the velocity (second row) at time $t = 0.1$ with a space step $\Delta x = 10^{-2}$ obtained using different solvers. The simulations are performed with a CFL parameter set to 1 for the first column and with a CFL parameter set to 0.1 for the second column. The CPR scheme is computed using the CFL condition (2.4) with $\gamma = 1$ and $\gamma = 100$. Note in such configuration, the time step of the schemes are comparable, i.e. $\Delta t \approx 10^{-3}$ for a CFL parameter set to 1. However, this is a particular case and if the water level in the right part is small, the time step of the CPR scheme will be impacted, i.e. it will be smaller. On the contrary, if the global water level is larger, the time step of the CPR scheme will be larger.

In rarefaction areas and for CFL parameter set to 1, the CPR scheme leads to similar result than the less diffusive first order Godunov schemes such as Roe solver with entropic correction or HLL solver. When the CFL parameter is smaller, the CPR scheme becomes less diffusive and tends to similar result than Lax-Wendroff while classical first order Godonov schemes become more diffusive. In shock areas, the CPR scheme with $\gamma = 1$ presents oscillations which recalls the dispersive oscillations of the Lax-Wendroff scheme. Note that the smaller the CFL parameter is, the larger the amplitudes of the oscillations are. Using larger regularization parameter $\gamma = 100$,

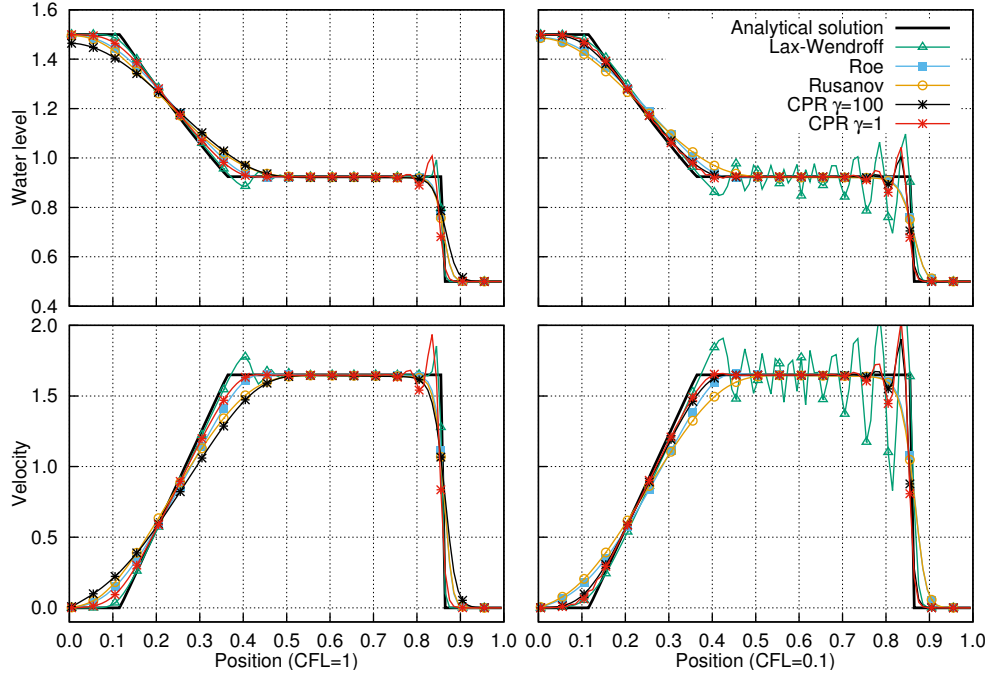


FIG. 2. Dam break simulation: Comparison between the CPR scheme ($\gamma = 1$ and $\gamma = 100$), Roe scheme and Lax-Wendroff scheme. Water elevation (first row) and velocity (second row) at time $t = 0.1$ with a CFL parameter set to 1 (first column) and 0.1 (second column), and a space step $\Delta x = 10^{-2}$.

the amplitudes of the oscillations decrease. Unfortunately, in the rarefaction areas the numerical diffusion become larger when the regularization parameter γ increase. However, the regularization parameter γ can be defined locally in function of the flow. The regularization parameter γ is estimated to ensure the dissipation of mechanical energy, which is preserved by the model $M_{t,\varepsilon}$ except in the shock areas, where the mechanical energy is dissipated. Then the value of the regularization parameter γ can be adapted in the shock areas to dissipate as much mechanical energy as the continuous model.

4.4. Lock exchange simulation. This test case is the simulation of the lock exchange experiment with the multilayer shallow water model. It is similar to the simulation of the dam break presented in section 4.3 with a second layer above such that the free surface is flat at the initial time. For more details about the test case and the physical interpretation of it, we refer to [19] and its references. More precisely the initial condition is given by

$$h_2^0(x) = \begin{cases} 1.5 & , \text{if } x < 0.5 \\ 0.5 & , \text{elsewhere.} \end{cases}, \quad h_1^0(x) = \begin{cases} 0.5 & , \text{if } x < 0.5 \\ 1.5 & , \text{elsewhere.} \end{cases}$$

and $u_1^0 = u_2^0 = z_b = 0$. We compare the CPR scheme ($\gamma = 1$ and $\gamma = 10$), the Lax-Wendroff scheme for the coupled bi-layer model, the Roe solver using the uncoupled treatment [9] and the Rusanov solver for the coupled bi-layer model. The simulations of this section are performed with a space step set to $\Delta x = 5 \cdot 10^{-3}$.

4.4.1. Large density ratio $\frac{\rho_2 - \rho_1}{\rho_2} = \frac{1}{2}$. Fig. 3 shows the interface levels and the velocity profiles for a density ratio set to $\frac{\rho_2 - \rho_1}{\rho_2} = \frac{1}{2}$. Except for the CPR scheme with the regularization parameter $\gamma = 10$ where the time step is slightly smaller $\Delta t \approx 10^{-4}$, the time steps used for all the schemes are close to $\Delta t \approx 5 \cdot 10^{-4}$. We can clearly identify the four waves of the Riemann problem corresponding to the initial condition. Remark that discontinuities appear in both layer thickness at the same position. In such configuration, the definition of the non-conservative product $\rho_i \nabla \phi_i$ is not clear and the solution could be not unique, see [2].

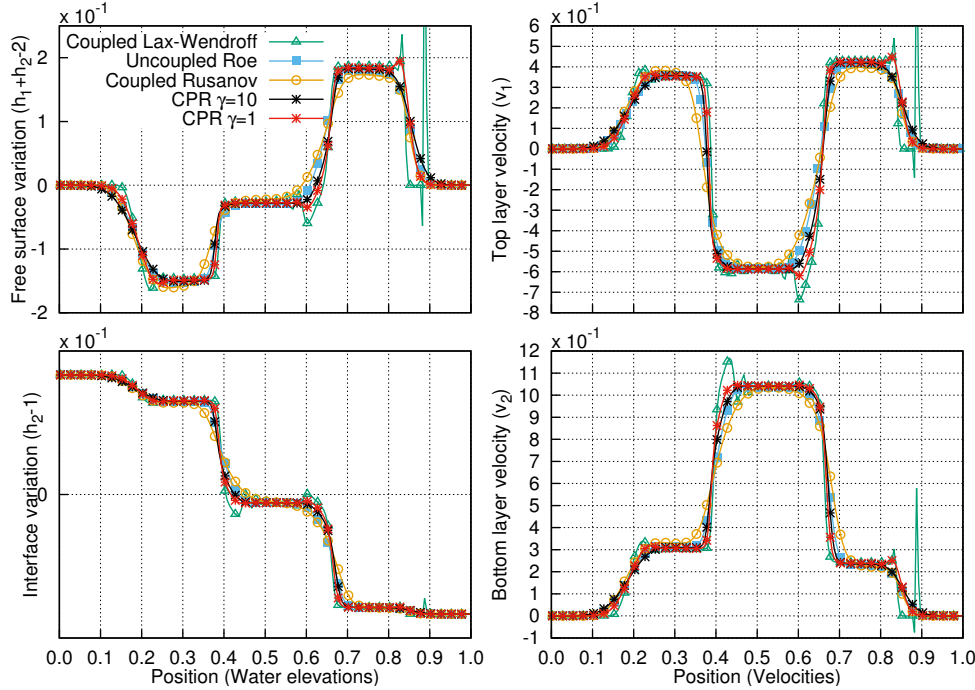


FIG. 3. *Lock exchange simulation: Comparison between the CPR scheme ($\gamma = 1$ and $\gamma = 10$) and classical Godunov schemes using coupled or uncoupled strategies with large density ratio ($\frac{\rho_2 - \rho_1}{\rho_2} = \frac{1}{2}$) at time $t = 0.08$ with $\Delta x = 5 \cdot 10^{-3}$.*

4.4.2. Small density ratio $\frac{\rho_2 - \rho_1}{\rho_1} = 10^{-4}$. Fig. 4 shows the interface levels and the velocity profiles for a very small density variation, i.e. $\frac{\rho_2 - \rho_1}{\rho_1} = 10^{-4}$. The time step used for the uncoupled Roe and the coupled Rusanov solver are still the same $\Delta t \approx 5 \cdot 10^{-4}$. The Lax-Wendroff scheme require a smaller time step to give the results presented in Fig. 4, i.e. $\Delta t \approx 10^{-4}$. With larger time step, the oscillations are much larger and the result becomes unreadable. The CPR scheme required a larger time step to satisfy the CFL condition (2.4). However the result obtained with a large time step is very diffusive. The results plotted in Fig. 4 used a time step of $\Delta t \approx 10^{-3}$.

Since the interactions between the layers are importante, the uncoupled treatment is no longer valuable, see [9]. The free surface is almost flat and the velocities of each layer are very small. More precisely the two faster waves observed in Fig. 3 disappear and the internal waves celerities are very small. In such regime, the Rusanov solver used for the coupled system is clearly very diffusive. The interface obtained with the

CPR scheme is in good agreement with the Lax-Wendroff scheme used for the coupled system. However, the result of the Lax-Wendroff scheme presents perturbations for all the degrees of freedom, i.e. the free surface, the interface between the layers and the velocities. This perturbation comes from the dispersive effect of the scheme and make the scheme useless for quantitative analysis. The solution observed is very close to the solution of the wave equations $M_{\tau,0}$ for the layer thickness, and the velocities are close to the one obtained with the rigid-lip model $M_{t,0}$, i.e. $h_1 u_1 = -h_2 u_2$.

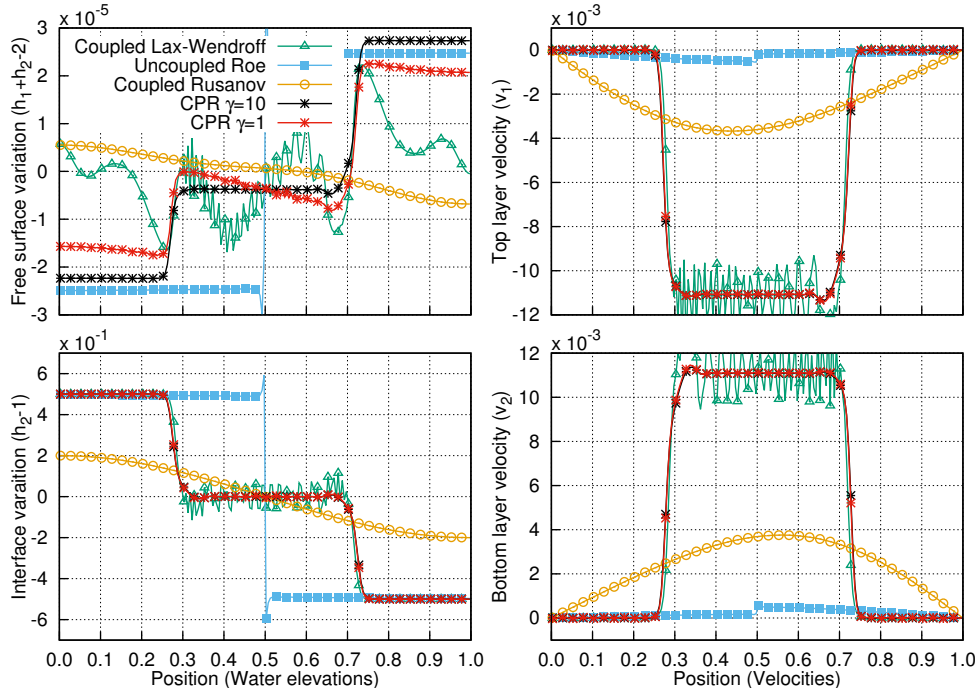


FIG. 4. Lock exchange simulation: Comparison between the CPR scheme ($\gamma = 1$, $\Delta t = 10^{-3}$) and classical Godunov schemes ($\Delta t = 5 \cdot 10^{-4}$) with very small density variation ($\frac{\rho_2 - \rho_1}{\rho_1} = 10^{-4}$) at time $t = 10$ with $\Delta x = 5 \cdot 10^{-3}$.

5. Conclusion. In the current paper, a new numerical scheme for advection equation with strong irrotational force in multi-dimensional framework is proposed and analyzed. The numerical scheme is applicable to a large classe of models of continuum mechanics satisfying an energy conservation. More precisely, the model is particularly well adapted to system of fluids and deals with the non-conservative interactions. Several numerical illustrations are presented in the context of multilayers shallow water model. The main avantages of the method is its strong robustness. The numerical strategy is accurate in the limit where the potential forces are large in front of the advection terms, the so-called low-Mach number regime or low-Froude number regime depending on the applications. We shows the dissipation of the total energy, acting as a mathematical entropy, even using a large time step, i.e. the time step is not depending on the celerity of the potential waves. The numerical results show that the solution can be improve without finer space discretization by reducing the time step, which is not true for classical Godunov schemes. In addition, the numerical strategy proposed does not required the estimation of eigenvalues of the system, which is very

hard when the system of equations become large. Note that the method satisfies the classical properties required for the computation of flow such that positivity, conservation of the total momentum, conservation of the steady state at rest and entropy dissipation. However, in the current version, the numerical scheme is not able to simulate vacuum/dry areas. The CFL condition required to ensure stability leads to vanishing time step in such regions. In addition, numerical experiments show the presence of oscillations in the vicinity of shock. The regularization parameter introduce in the scheme can correct this drawback but a fine analysis is required. Further works will reply to this questions. In addition, an extension to the case where the potentials of the forces are not an explicit function of the mass, for example for the non-isentropic Euler equations or the multi-polar Euler-Poisson equation, will be pertinent for enlarge the applicability of the method.

Acknowledgements. This research is part of a collaborative program with the French Naval Hydrographic and Oceanographic Service. Authors thank R. Baraille for many fruitful discussions and F. Couderc for his kind advices.

REFERENCES

- [1] ABGRALL, R., AND KARNI, S. Two-layer shallow water system: a relaxation approach. *SIAM J. Sci. Comput.* *31* (2009), 1603–1627.
- [2] ANDRIANOV, N. Performance of numerical methods on the non-unique solution to the riemann problem for the shallow water equations. *International Journal for Numerical Methods in Fluids* *47*, 8-9 (2005), 825–831.
- [3] AUDUSSE, E. A multilayer saint-venant model: derivation and numerical validation. *Discrete Contin. Dyn. Syst. Ser. B* *5* (2005), 189–214.
- [4] AUDUSSE, E., BOUCHUT, F., BRISTEAU, M.-O., KLEIN, R., AND PERTHAME, B. A fast and stable well-balanced scheme with hydrostatic reconstruction for shallow water flows. *SIAM J. Sci. Comput.* *25*, 6 (2004), 2050–2065.
- [5] BEDFORD, A., AND DRUMHELLER, D. S. Theories of immiscible and structured mixtures. *International Journal of Engineering Science* *21*, 8 (1983), 863–960.
- [6] BERMUDEZ, A., AND VAZQUEZ, M. E. Upwind methods for hyperbolic conservation laws with source terms. *Comput. & Fluids* *23*, 8 (1994), 1049–1071.
- [7] BERNARD, M., DELLACHERIE, S., FACCANONI, G., GREC, B., AND PENEL, Y. Study of a low mach nuclear core model for two-phase flows with phase transition I: stiffened gas law. *ESAIM Math. Model. Numer. Anal.* *48* (11 2014), 1639–1679.
- [8] BIANCHINI, S. On the riemann problem for non-conservative hyperbolic systems. *Arch. Ration. Mech. Anal.* *166*, 1 (2003), 1–26.
- [9] BOUCHUT, F., AND DE LUNA, T. M. An entropy satisfying scheme for two-layer shallow water equations with uncoupled treatment. *ESAIM Math. Model. Numer. Anal.* *42* (2008), 683–698.
- [10] BOUCHUT, F., ZEITLIN, V., ET AL. A robust well-balanced scheme for multi-layer shallow water equations. *Discrete Contin. Dyn. Syst. Ser. B* *13*, 4 (2010), 739–758.
- [11] CHAINAIS-HILLAIRET, C., PENG, Y.-J., AND VIOLET, I. Numerical solutions of euler–poisson systems for potential flows. *Appl. Numer. Math.* *59*, 2 (2009), 301–315.
- [12] CHEN, F. F., AND SMITH, M. D. *Plasma*. Wiley Online Library, 1984.
- [13] DE SAINT-VENANT, A.-J.-C. B. Théorie du mouvement non permanent des eaux, avec application aux crues des rivières et à l’introduction des marées dans leurs lits. *C.R. Acad. Sci. Paris* *73* (1871), 147–154.
- [14] DELLACHERIE, S. Analysis of godunov type schemes applied to the compressible euler system at low mach number. *J. Computational Phys.* *229* (2010), 978–1016.
- [15] DUCHÈNE, V. Asymptotic shallow water models for internal waves in a two-fluid system with a free surface. *SIAM J. Math. Anal.* *42* (2010), 2229–2260.
- [16] GAVRILYUK, S., AND GOUIN, H. A new form of governing equations of fluids arising from hamilton’s principle. *Internat. J. Engrg. Sci.* *37*, 12 (1999), 1495–1520.
- [17] GREENBERG, J. M., AND LEROUX, A.-Y. A well-balanced scheme for the numerical processing of source terms in hyperbolic equations. *SIAM J. Numer. Anal.* *33*, 1 (1996), 1–16.

- [18] GRENIER, N., VILA, J.-P., AND VILLEDIEU, P. An accurate low-mach scheme for a compressible two-fluid model applied to free-surface flows. *J. Computational Phys.* 252 (2013), 1–19.
- [19] ILCAK, M., ADCROFT, A. J., GRIFFIES, S. M., AND HALLBERG, R. W. Spurious diapycnal mixing and the role of momentum closure. *Ocean Modelling* 45–46, 0 (2012), 37–58.
- [20] ISOZAKI, H. Singular limits for the compressible euler equation in an exterior domain. *J. Reine Angew. Math.* 381 (1987), 1–36.
- [21] ISOZAKI, H. Wave operators and the incompressible limit of the compressible euler equation. *Comm. Math. Phys.* 110, 3 (1987), 519–524.
- [22] ISOZAKI, H., ET AL. Singular limits for the compressible euler equation in an exterior domain. ii. bodies in a uniform flow. *Osaka J. Math.* 26, 2 (1989), 399–410.
- [23] KLAINERMAN, S., AND MAJDA, A. Singular limits of quasilinear hyperbolic systems with large parameters and the incompressible limit of compressible fluids. *Comm. Pure Appl. Math.* 34, 4 (1981), 481–524.
- [24] KLAINERMAN, S., AND MAJDA, A. Compressible and incompressible fluids. *Communications on Pure and Applied Mathematics* 35, 5 (1982), 629–651.
- [25] KLEIN, R., AND VATER, S. Mathematische modellierung in der klimaforschung. *Freie Universität Berlin, Fachbereich Mathematik und Informatik. Vorlesungsskript* (2003).
- [26] LIU, M.-S., AND STEFFEN JR, C. J. A new flux splitting scheme. *J. Comput. Phys.* 107, 1 (1993), 23–39.
- [27] LISKA, R., AND WENDROFF, B. Analysis and computation with stratified fluid models. *J. Comput. Phys.* 137, 1 (1997), 212–244.
- [28] LONG, R. R. Long waves in a two-fluid system. *Journal of Meteorology* 13, 1 (1956), 70–74.
- [29] MÉTIVIER, G., AND SCHOCHET, S. The incompressible limit of the non-isentropic euler equations. *Arch. Ration. Mech. Anal.* 158, 1 (2001), 61–90.
- [30] MONJARRET, R. Local well-posedness of the multi-layer shallow water model with free surface. To appear.
- [31] NATALINI, R., RIBOT, M., AND TWAROGOWSKA, M. A well-balanced numerical scheme for a one dimensional quasilinear hyperbolic model of chemotaxis. *Commun. Math. Sci.* 12, 1 (2014), 13–39.
- [32] NOELLE, S., PANKRATZ, N., PUPPO, G., AND NATVIG, J. R. Well-balanced finite volume schemes of arbitrary order of accuracy for shallow water flows. *J. Comput. Phys.* 213, 2 (2006), 474–499.
- [33] OVSYANNIKOV, L. Two-layer “shallow water” model. *J. Appl. Mech. Tech. Phys.* 20, 2 (1979), 127–135.
- [34] PARISOT, M., AND VILA, J.-P. Numerical scheme for multilayer shallow-water model in the low-froude number regime. *C.R. Acad. Sci. Paris, Ser. I* 352 (2014), 953–957.
- [35] PERTHAME, B., AND SIMEONI, C. A kinetic scheme for the saint-venant system with a source term. *Calcolo* 38, 4 (2001), 201–231.
- [36] RAVIART, P.-A. *Numerical approximation of hyperbolic systems of conservation laws*, vol. 118. Springer, 1996.
- [37] REZNIK, G., ZEITLIN, V., AND BEN JELLOUL, M. Nonlinear theory of geostrophic adjustment. part 1. rotating shallow-water model. *J. Fluid Mech.* 445 (2001), 93–120.
- [38] SCHIJF, J., AND SCHÖNFLED, J. Theoretical considerations on the motion of salt and fresh water. IAHR, 1953.
- [39] SERRIN, J. Mathematical principles of classical fluid mechanics. In *Fluid Dynamics I/Strömungsmechanik I*. Springer, 1959, pp. 125–263.
- [40] SHEN, J. Pseudo-compressibility methods for the unsteady incompressible navier-stokes equations. *Proceedings of the 1994 Beijing symposium on nonlinear evolution equations and infinite dynamical systems* (1997), 68–78.
- [41] SLEMROD, M. Dynamic phase transitions in a van der waals fluid. *J. Differential Equations* 52, 1 (1984), 1–23.
- [42] STOKER, J. J. *Water waves: The mathematical theory with applications*, vol. 36. John Wiley & Sons, 2011.
- [43] STRAUSS, W. A. *Partial Differential Equations: An Introduction*. John Wiley, 1992.
- [44] WIJNGAARDEN, L. v. On the equations of motion for mixtures of liquid and gas bubbles. *J. Fluid Mech.* 33, 03 (1968), 465–474.